AN ABSTRACT OF THE THESIS OF

Marvin Minei for the degree of Master of Science in Mathematics presented on August 8, 1988.

Title: An Analysis Of Accuracy Of Finite Difference And Finite Element Methods For The Wave Equation

Redacted for Privacy

Abstract Approved : _____
Robert L. Higdon

In this paper, Fourier analysis is used to investigate various approximation methods for the one- and two-dimensional wave equations. The spatial derivatives are approximated by the second order centered finite difference method, the linear and quadratic finite element methods, and the fourth order centered finite difference method. The approximation schemes thus obtained shall be continuous in time. Using Fourier analysis, their general solutions can be obtained. Group velocities of these solutions are then compared to the group velocity of the solution to the wave equation. These comparisons will yield a measure of accuracy for the approximation schemes. Finally, we obtain numerical computing schemes by using the second order centered finite difference method in time. Group velocities for these fully discrete schemes

are also analyzed and the Courant number for each computing scheme will be shown to have an effect on its accuracy. In the one- and two-dimensional case, numerical results are given to back up the analysis.

An Analysis Of Accuracy Of Finite Difference And Finite Element Methods For The Wave Equation

by

Marvin Minei

A THESIS

submitted to

Oregon State University

in partial fulfillment of

the requirements of the

degree of

Master of Science

Completed August 8, 1988

Commencement June 1989

APPROVED :

Redacted for Privacy

Associate Professor of Mathematics in charge of major

Redacted for Privacy

Chairman of Department of Mathematics

Redacted for Privacy

Dean of Graduate School

Date thesis is presented August 8, 1988

Typed by the author Marvin K. Minei

ACKNOWLEGEMENTS

First of all, I would like to thank Dr. Robert L. Higdon for helping me to complete this paper. His patience and supervision of my work was invaluable.

Secondly, I would like to thank my parents and grandparents for everything they have ever done for me.

TABLE OF CONTENTS

LIST OF FIGURES

AN ANALYSIS OF ACCURACY OF FINITE DIFFERENCE AND FINITE ELEMENT METHODS FOR THE WAVE EQUATION

1. INTRODUCTION

We will use the following methods to approximate the spatial derivatives in both the one- and two-dimensional wave equations.

1. The second order centered finite difference method

2. The linear finite element method

3. The quadratic finite element method

4. The fourth order centered finite difference method (obtained through Richardson extrapolation).

This will yield four different time continuous approximation schemes. Although they cannot be used to compute numerical approximations, their general solutions will be studied to determine the degree of accuracy methods 1 through 4 will yield in the approximation of the spatial derivatives.

For each of the schemes, we obtain a form for its general solution using Fourier analysis. The group velocities of these general solutions will then be compared to the group velocity of the solution to the wave

equation. It is in this fashion that we will determine a level of accuracy each method will provide.

Numerical computing schemes will be obtained by implementing the second order centered finite difference method in time to each of the four time continuous schemes. Again, we will determine the accuracy levels of each numerical computing scheme by comparing the group velocities of their general solutions to the group velocity of the solution to the wave equation. The accuracy of each scheme will depend on the value of the Courant number chosen.

It should be noted that using a different approximation method in time would result in different numerical computing schemes and different levels of accuracy.

The remainder of this paper is divided into fifteen sections. Sections 4 through 9 deal with approximation methods applied to the 1-D wave equation, and sections 10 through 16 are on approximation methods applied to the 2-D wave equation. Section 2 introduces the idea of group and phase velocity for a one- dimensional propagating wave. Section 3 discusses the solutions to the wave equation in 1-D. Sections 4 through 8 present the following approximation methods (in order of their appearance): the second order centered finite difference method, the linear finite element method, the quadratic finite element method, the revised linear finite element method, and the fourth order

centered finite difference method. Section 9 gives a brief conclusion of the results from sections 4 to 8. Section 10 introduces the idea of group and phase velocity for a two-dimensional propagating wave. Section 11 is a discussion on the wave equation in 2-D. Sections 12 through 15 are on the second order centered finite difference method, the linear finite element method, the revised linear finite element method, and the fourth order centered finite difference method, respectively. Section 16 is a conclusion on the findings on sections 12 to 15.

2. GROUP AND PHASE VELOCITY IN ONE DIMENSION

Consider a propagating wave of the form

$$u(x,t) = \int_a^b f(k)\cdot e^{i(kx-\omega t)}\, dk, \qquad (2.1)$$

where f is a bounded real-valued amplitude function and $\omega=\omega(k)$. We will define and discuss the group and phase velocity functions of u. In a physical setting, only the real part of u would be used, but complex exponential notation is used here for convenience.

Choose k_0 between a and b. We will require that (b−a) be small compared to $|k_0|$. Define $\omega_0=\omega(k_0)$ and consider

$$u(x,t) = e^{i(k_0x-\omega_0t)}\cdot\int_a^b f(k)\cdot e^{i[(k-k_0)x-(\omega-\omega_0)t]}\, dk.$$

By Taylor's theorem,

$$\omega(k)-\omega(k_0) = (k-k_0)\cdot\omega'(k_0) + O(k-k_0)^2$$

and so

$$u(x,t) \approx e^{i(k_0x-\omega_0t)}\cdot\int_a^b f(k)\cdot e^{i(k-k_0)[x-\omega'(k_0)t]}\, dk.$$

Consider the real part of this equation,

$$\cos(k_0x-\omega_0t)\cdot\int_a^b f(k)\cdot\cos(k-k_0)[x-\omega'(k_0)t]\, dk$$

$$-\sin(k_0x-\omega_0t)\cdot\int_a^b f(k)\cdot\sin(k-k_0)[x-\omega'(k_0)t]\, dk. \qquad (2.2)$$

Define $F(x-\omega'(k_0)t)$ to be the first integral in (2.2). For fixed t, consider

$$\frac{\partial}{\partial x} F(x-\omega'(k_0)t) = -\int_a^b f(k)\cdot(k-k_0)\cdot\sin(k-k_0)[x-\omega'(k_0)t]\, dk.$$

Thus, for M an upper bound for $|f|$ on $[a,b]$, we get

$$\left|\frac{\partial}{\partial x}F(x-\omega'(k_0)t)\right| \leq M\cdot\int_a^b |k-k_0|\, dk$$

$$\leq M\cdot\max|k-k_0|\cdot(b-a).$$

Therefore, for (b-a) small enough, we can make

$$\left|\frac{\partial}{\partial x} F(x-\omega'(k_0)t)\right| \ll |k_0| \tag{2.3}$$

while

$$\max\left|\frac{\partial}{\partial x}\cos(k_0x-\omega_0t)\right| = |k_0|. \tag{2.4}$$

We interpret this as follows. Consider the first term in (2.2),

$$\cos(k_0x-\omega_0t)\cdot F(x-\omega'(k_0)t). \tag{2.5}$$

Fix t. By (2.3) and (2.4), the maximum value of $\left|\frac{\partial}{\partial x}F(x-\omega'(k_0)t)\right|$ is always small compared to the maximum value of the derivative with respect to x of the cosine term. Thus, we expect the graph of F to be a slowly varying one relative to the graph of the cosine term. The graph of (2.5) then is the graph of the cosine term embedded in a wave envelope of the form from the graph of F. The veloci-

ty of this envelope, i.e., the velocity of F, is what we will define to be the group velocity Cg, of (2.5). Since the velocity of F is $\omega'(k_0)$, $Cg=\omega'(k_0)$. The velocity of the wave in the envelope will be defined as the phase velocity C_p, of (2.5). Since the velocity of this wave is the velocity of the cosine term in (2.5), we have $C_p=\omega_0/k_0$.

Similar arguments can be applied to the second part of (2.2). The real part of u (and the imaginary part,also) then has a group velocity $Cg=\omega'(k_0)$.

As an example, consider u(x,t) with f(k)=1 on [a,b] and zero elsewhere. Then, (2.2) becomes

$$\cos(k_0x-\omega_0t)\cdot \frac{1}{x-\omega'(k_0)t}\cdot [\ \sin(b-k_0)(x-\omega'(k_0)t) - \sin(a-k_0)(x-\omega'(k_0)t)\ ] + \sin(k_0x-\omega_0t)\cdot \frac{1}{x-\omega'(k_0)t}\cdot [\ \cos(b-k_0)(x-\omega'(k_0)t) - \cos(a-k_0)(x-\omega'(k_0)t)\ ]. \tag{2.6}$$

We write (2.6) in a simpler form that can be easily sketched. Define

$$\begin{aligned} A &= (a-k_0)(x-\omega'(k_0)t) \\ B &= (b-k_0)(x-\omega'(k_0)t) \\ \alpha &= \frac{B+A}{2} \\ \beta &= \frac{B-A}{2}\ . \end{aligned}$$

Then, (2.6) becomes

$$\cos(k_0x-\omega_0t)\cdot \frac{1}{x-\omega'(k_0)t}\cdot [\ \sin(\alpha+\beta) - \sin(\alpha-\beta)\ ]$$

$$+\ \sin(k_0x-\omega_0t)\cdot \frac{1}{x-\omega'(k_0)t}\cdot [\ \cos(\alpha+\beta) - \cos(\alpha-\beta)\ ]$$

or

$$\frac{1}{x-\omega'(k_0)t}\cdot \sin\beta\cdot 2\cos(k_0x-\omega_0t+\alpha) \quad . \tag{2.7}$$

It is easy to check that $\sin\beta$ has wave number $\frac{1}{2}(b-a)$ and the cosine term has wave number $\frac{1}{2}(b+a)$. The first two factors of (2.7) will make up the wave envelope that travels with a velocity $\omega'(k_0)$.

At $x= \omega'(k_0)t$, (2.7) appears to have a singularity but it is easy to see that

$$\lim_{x\to\omega'(k_0)t} \frac{\sin\beta}{x-\omega'(k_0)t}$$

exists. Using the fact that

$$\lim_{\theta\to 0} \frac{\sin\theta}{\theta} = 1$$

and that

$$\frac{\sin\beta}{x-\omega'(k_0)t} = \frac{\sin\frac{1}{2}(b-a)(x-\omega'(k_0))t}{x-\omega'(k_0)t}$$

$$= \frac{\frac{1}{2}(b-a)\cdot \sin\frac{1}{2}(b-a)(x-\omega'(k_0)t)}{\frac{1}{2}(b-a)(x-\omega'(k_0)t)} \quad ,$$

we see that the limit is $\frac{1}{2}(b-a)$. Figure 2.1 is a graph of (2.7) where a=20, b=25, k_0=22.5, and t=0. The velocity of the envelope is $\omega'(k_0)$ and the velocity of the wave in the envelope is $\frac{\omega(k_0)}{k_0}$. If we observe (2.7) as t increases from zero, it is possible that the envelope will travel in one direction while the wave in the envelope will travel in the opposite direction.

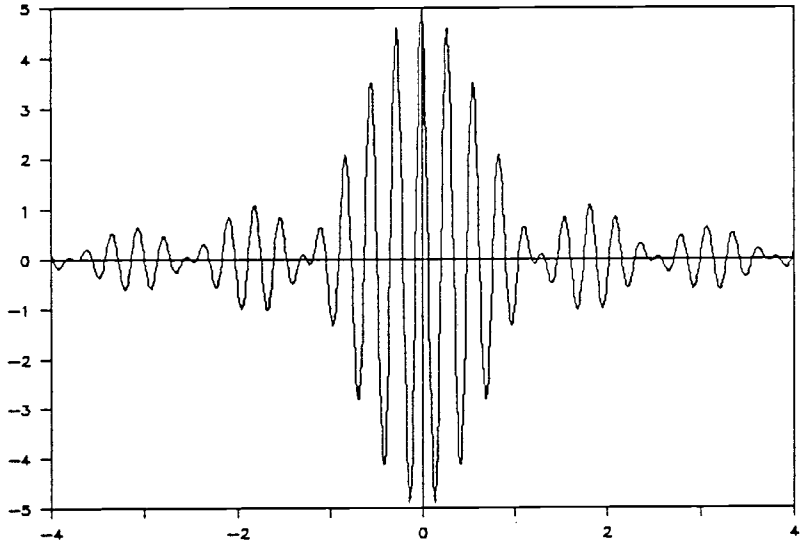

Figure 2.1. Graph of a propagating wave. The graph of (2.7) where a=20, b=25, k_0=22.5, and t=0.

Next, consider a more general form for (2.1), viz., where the size of (b−a) is arbitrary. We will deal with u in the following manner. Divide [a,b] into tiny intervals by

$$a=\alpha_0 < \alpha_1 < \alpha_2 < \ . \ . \ . < \alpha_{m-1} < b=\alpha_m$$

and consider

$$u(x,t) = \int_{\alpha_0}^{\alpha_1} f(k)\cdot e^{i(kx-\omega t)}\, dk + \ . \ . \ . \int_{\alpha_{m-1}}^{\alpha_m} f(k)\cdot e^{i(kx-\omega t)}\, dk \ . \tag{2.8}$$

Each integral represents a travelling wave, with the

jth integral having the group velocity $\omega'(k_j)$, $\alpha_{j-1} \leq k_j \leq \alpha_j$. Thus, u can be thought of as a superposition of these waves, each travelling with a particular group velocity. Over time, the slower superposed waves will fall behind the others while the faster waves will move ahead. Because of this, we expect u to be a travelling wave which will change in appearance as t increases from zero. In an intuitive sense, we say that u is dispersing over time and it is for this reason that the equation relating ω and k is called the dispersion relation for u. If ω is a linear function of k, $\omega'(k)$ will be constant and in such a case we expect u never to disperse since all the superposed waves of (2.8) will have equal group velocities.

3. SOLUTIONS TO THE ONE-DIMENSIONAL WAVE EQUATION

When we begin the analysis of the various approximation methods in one and two dimensions, it will be important to know some general behavior of solutions to the wave equation.

Consider the one-dimensional wave equation for some given initial conditions

$$u_{tt} = c^2 \cdot u_{xx}.$$

We will consider only initial value problems and not initial boundary value problems for the wave equation because it will simplify our later analysis quite a bit. According to D'Alembert, there exist functions A and B, their exact forms depending on initial conditions, such that

$$u(x,t) = A(x+ct) + B(x-ct).$$

We can think of u(x,t) as made up of two waves, one travelling with velocity c and the other travelling with velocity -c. The solution to an initial-value problem can also be represented in an integral form with the dispersion relation

$$\omega^2 = c^2 \cdot k^2.$$

Since $\omega'(k) = \pm c$, no dispersion will occur.

In the next sections, we begin looking at various numerical schemes where dispersion will occur. The extent that dispersion occurs is the extent that the scheme is im-

perfect (this being in the cases where the scheme is non-dissipative). For more information on this subject, see [Trefethen]. For a general discussion of dispersion in physical systems, see [Lighthill] and [Whitham]. The two-dimensional case will be considered later.

4. THE SECOND ORDER CENTERED FINITE DIFFERENCE METHOD IN 1–D

We are now ready to begin our analysis in one dimension. The first approximation method to be considered is the second order centered finite difference method. In this section, we will be considering the initial value problem involving the wave equation instead of the initial boundary value problem. In practice, we could compute solutions only to IBVP's but IVP's are considered in order to eliminate the need to incorporate effects of boundedness into the analysis.

Let $u(x,t)$ represent a solution to the 1-D wave equation. We will approximate u at the points $x_j = j\cdot\Delta x$ where j is an integer.

Let $u_j(t)$ approximate $u(j\cdot\Delta x,t)$ and define

$$D_x^+ u_j(t) = \frac{1}{\Delta x}\left(u_{j+1}(t) - u_j(t) \right)$$

$$D_x^- u_j(t) = \frac{1}{\Delta x}\left(u_j(t) - u_{j-1}(t) \right).$$

So,

$$D_x^+ D_x^- u_j(t) = \frac{1}{\Delta x^2}\left(u_{j+1}(t) - 2\cdot u_j(t) + u_{j-1}(t) \right).$$

The second order centered finite difference approximation scheme is

$$\left(\frac{c}{\Delta x}\right)^2 \cdot \left(u_{j+1}(t) - 2\cdot u_j(t) + u_{j-1}(t) \right) - u_j''(t) = 0. \quad (4.1)$$

We call this a second order scheme because of the following reason. Consider a function $f(x)$. By Taylor's theo-

rem, for x_0 fixed,

$$f(x) = f(x_0) + (x-x_0)\cdot f'(x_0) + \frac{(x-x_0)^2}{2!}\cdot f''(x_0) + \frac{(x-x_0)^3}{3!}\cdot f^{(3)}(x_0) + \frac{(x-x_0)^4}{4!}\cdot f^{(4)}(\alpha)$$

where α is between x and x_0. First set x equal to $(x+x_0)$ and then $(x-x_0)$. Add the two equations to get

$$f''(x_0) = \frac{f(x_0+\Delta x) - 2\cdot f(x_0) + f(x_0-\Delta x)}{\Delta x^2} - \frac{\Delta x^2}{24}\cdot (f^{(4)}(\alpha) + f^{(4)}(\beta))$$

where α is between x_0 and $(x_0+\Delta x)$; β between $(x_0-\Delta x)$ and x_0. Since f and x_0 are both arbitrary,

$$u_{xx}(x,t) = \frac{u(x+\Delta x,t) - 2\cdot u(x,t) + u(x-\Delta x,t)}{\Delta x^2} + O(\Delta x)^2 .$$

Therefore,

$$\frac{1}{\Delta x^2}\cdot (u_{j+1}(t) - 2\cdot u_j(t) + u_{j-1}(t))$$

approximates $u_{xx}(j\cdot\Delta x,t)$ with an error of order two .

We will determine an integral form for $u_j(t)$, the solution to (4.1). This integral will be used to determine the accuracy level of (4.1) as an approximation scheme to the wave equation.

To determine a form for $u_j(t)$, we use Fourier analysis. Define a Fourier transform of the grid function by

$$\hat{u}(k\Delta x,t) = \Delta x\cdot \sum_{j=-\infty}^{\infty} u_j(t)\cdot e^{-ik\Delta xj}$$

$$= \sum_{j=-\infty}^{\infty} \left(\Delta x \cdot u_j(t) \right) \cdot e^{-ik\Delta x j} .$$

Think of this as a Fourier series expansion for $\hat{u}(k\Delta x,t)$ in $k\Delta x$. Since $\hat{u}$ has a period of 2π, we restrict $-\pi \leq k\Delta x \leq \pi$. If we regard $\Delta x \cdot u_j(t)$ as the coefficients in the series, then

$$\Delta x \cdot u_j(t) = \frac{1}{2\pi} \int_{-\pi}^{\pi} \hat{u}(k\Delta x,t) \cdot e^{ik\Delta x j} \, d(k\Delta x)$$

or

$$u_j(t) = \frac{1}{2\pi} \int_{-\pi/\Delta x}^{\pi/\Delta x} \hat{u}(k\Delta x,t) \cdot e^{ik\Delta x j} \, dk \quad . (4.2)$$

To determine the form of $\hat{u}$, put (4.2) into (4.1) and assume the second time derivative and integral signs can be switched. Then

$$0 = \frac{1}{2\pi} \int_{-\pi/\Delta x}^{\pi/\Delta x} [(\tfrac{c}{\Delta x})^2 \cdot (e^{ik\Delta x} - 2 + e^{-ik\Delta x}) \cdot \hat{u}(k\Delta x,t) - \hat{u}_{tt}] \cdot e^{i(j\Delta x)k} \, dk .$$

We write the term in brackets as [...]. Rewrite the equation as

$$0 = \frac{\Delta x}{2\pi} \int_{-\pi}^{\pi} [...] \cdot e^{ijk\Delta x} \, d(k\Delta x) .$$

Think of the right side as the coefficients for the Fourier series to [...]. But if each coefficient is zero, the series sums up to zero, i.e.,

$$0 = (\tfrac{c}{\Delta x})^2 \cdot (e^{ik\Delta x} - 2 + e^{-ik\Delta x}) \cdot \hat{u}(k\Delta x,t) - \hat{u}_{tt} .$$

Solving for $\hat{u}$ gives

$$\hat{u}(k\Delta x,t) = A(k) \cdot e^{-i\omega t} + B(k) \cdot e^{i\omega t}$$

with

$$\omega = \omega(k) = \left(\frac{c}{\Delta x}\right)\cdot\sqrt{2\,(1-\cos k\Delta x)}\ .$$

Define ω_1 and ω_2 as follows,

$$\omega_1 = \omega_1(k) = \begin{cases} \left(\frac{c}{\Delta x}\right)\cdot\sqrt{2\,(1-\cos k\Delta x)} & \text{for} \quad 0 \le k\Delta x \le \pi \\ -\left(\frac{c}{\Delta x}\right)\cdot\sqrt{2\,(1-\cos k\Delta x)} & \text{for} \quad -\pi \le k\Delta x \le 0 \end{cases} \tag{4.3}$$

$$\omega_2 = \omega_2(k) = \begin{cases} -\left(\frac{c}{\Delta x}\right)\cdot\sqrt{2\,(1-\cos k\Delta x)} & \text{for} \quad 0 \le k\Delta x \le \pi \\ \left(\frac{c}{\Delta x}\right)\cdot\sqrt{2\,(1-\cos k\Delta x)} & \text{for} \quad -\pi \le k\Delta x \le 0. \end{cases} \tag{4.4}$$

Thus, we can write $u_j(t)$ as

$$u_j(t) = \frac{1}{2\pi}\int_{-\pi/\Delta x}^{\pi/\Delta x} A(k)\cdot e^{i(k\Delta x)j - i\omega_1 t}\,dk + \frac{1}{2\pi}\int_{-\pi/\Delta x}^{\pi/\Delta x} B(k)\cdot e^{i(k\Delta x)j - i\omega_2 t}\,dk.$$

The equation (4.3) is the dispersion relation for the first integral in $u_j(t)$ and (4.4) is the dispersion relation for the second integral.

Here is how we will determine the behavior of $u_j(t)$. Divide $[-\frac{\pi}{\Delta x}, \frac{\pi}{\Delta x}]$ into really tiny intervals using the points

$$-\tfrac{\pi}{\Delta x} = a_0 < a_1 < \ldots < \alpha < 0 < \beta < \ldots < a_{m-1} < \tfrac{\pi}{\Delta x} = a_m$$

and divide $u_j(t)$ into a sum of integrals using these points. So,

$$u_j(t) = \frac{1}{2\pi}\Big[\int_{a_0}^{a_1} A(k)\cdot e^{i(k\Delta x)j - i\omega_1 t}\,dk + \int_{a_0}^{a_1} B(k)\cdot e^{i(k\Delta x)j - i\omega_2 t}\,dk$$

$$+ \ldots + \int_{a_{m-1}}^{a_m} A(k)\cdot e^{i(k\Delta x)j - i\omega_1 t}\,dk + \int_{a_{m-1}}^{a_m} B(k)\cdot e^{i(k\Delta x)j - i\omega_2 t}\,dk\Big]. \tag{4.5}$$

By previous work, if $[a_p, a_{p+1}] \neq [\alpha, \beta]$,

$$\int_{a_p}^{a_{p+1}} A(k)\cdot e^{i(k\Delta x)j - i\omega_1 t}\, dk + \int_{a_p}^{a_{p+1}} B(k)\cdot e^{i(k\Delta x)j - i\omega_2 t}\, dk$$

is a superposition of two wave trains, one with group velocity $\omega_1'(k_0)$, the other with group velocity $\omega_2'(k_0)$, $a_p < k_0 < a_{p+1}$. But consider the integrals

$$\int_{\alpha}^{\beta} A(k)\cdot e^{i(k\Delta x)j - i\omega_1 t}\, dk + \int_{\alpha}^{\beta} B(k)\cdot e^{i(k\Delta x)j - i\omega_2 t}\, dk. \qquad (4.6)$$

We cannot reference section 2 to conclude that they are both travelling with group velocities $\omega_1'(k_0)$ and $\omega_2'(k_0)$ respectively, with $\alpha \leq k_0 \leq \beta$. (Recall that section 2 required that $(\beta-\alpha)$ be small compared to $|k_0|$.) However, $\omega_1(k) \approx \omega_1'(0)\cdot k$ and $\omega_2(k) \approx \omega_2'(0)\cdot k$. Thus, $e^{i[kx-\omega_1(k)t]} \approx e^{ik[x-\omega_1'(0)t]}$ and $e^{i[kx-\omega_2(k)t]} \approx e^{ik[x-\omega_2'(0)t]}$. So, we can approximate (4.6) by

$$\int_{\alpha}^{\beta} A(k)\cdot e^{ik[\Delta x\cdot j - \omega_1'(0)t]}\, dk + \int_{\alpha}^{\beta} B(k)\cdot e^{ik[\Delta x\cdot j - i\omega_2'(0)t]}\, dk.$$

These two integrals are complex sinusoidal waves moving with velocities $\omega_1'(0) = c$ and $\omega_2'(0) = c$, respectively. In this case, the group and phase velocities are equal.

We interpret our findings. If we think of $u_j(t)$ as a sum of 2m integrals as in (4.5) (the number of integrals depending on how accurate an interpretation of $u_j(t)$ is needed) then $u_j(t)$ is a superposition of 2m waves where index j corresponds to both a rightgoing wave and a leftgo-

ing wave. The integrals with limits of integration spanning over zero will have group velocities very close to c and -c.

Consider Figure 4.1, the graph of (4.3). Keeping in mind that the value for m in (4.5) can be made as large as we want, we see that the superposing waves corresponding to k close to zero will have group velocities approximately equal to each other and in fact, approximately equal to c. But the superposing waves corresponding to k close to either $\frac{\pi}{\Delta x}$ or $-\frac{\pi}{\Delta x}$ will travel at a group velocity less than c. Thus, if we observe the first integral of $u_j(t)$ over time, the superposing waves with lower group velocities (i.e., shorter wavelengths) will lag behind and cause the integral to be dispersive in nature.

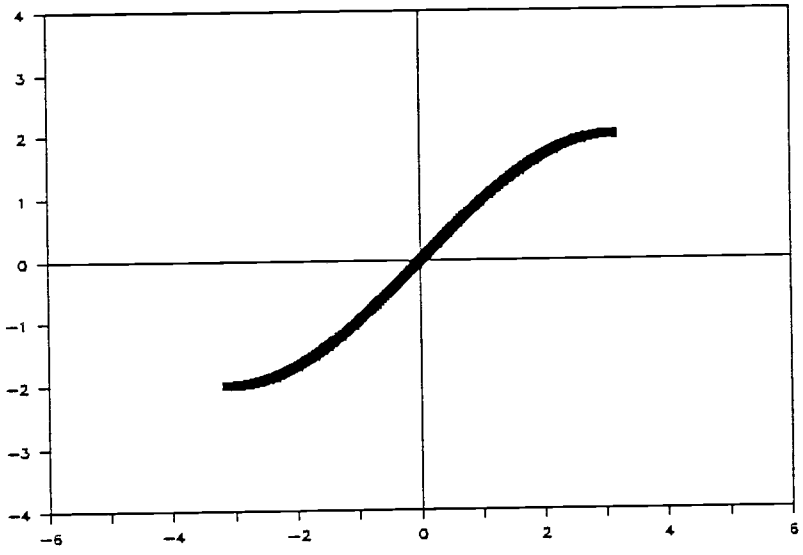

Figure 4.1. Dispersion relation for the first integral of $u_j(t)$. This is the graph of (4.3). It is plotted in the $(k\Delta x, \frac{\omega_1 \Delta x}{c})$-space where $-\pi \leq k\Delta x \leq \pi$. The slope of the curve at a point $(k\Delta x, \frac{\omega_1 \Delta x}{c})$ will give the group velocity (up to a multiplicative constant) for the superposed wave with wave number k. Near the origin, the curve is linear. Thus, waves with wave number k where $|k| \approx 0$ will travel with a group velocity about equal to c.

A similar argument can be applied to the second integral of $u_j(t)$ because the graph of (4.4) is just the negative of (4.3). We expect the second integral to be dispersive also, but travel in the opposite direction of the first integral. Thus, $u_j(t)$ is composed of two dispersive

waves that travel in opposite directions. Had the graphs of (4.3) and (4.4) been two straight lines each of slope $\pm c$, $u_j(t)$ would have been a perfect trace of $u(x,t)$.

Another way of investigating the rate of dispersion of $u_j(t)$ is to explicitly determine a relative group velocity error function for each of its integrals and observe the rate it goes to zero as k tends to zero. Consider the first integral of $u_j(t)$. The wave with wave number k has a group velocity

$$\omega_1'(k) = \begin{cases} \dfrac{c\cdot\sin k\Delta x}{\sqrt{2(1-\cos k\Delta x)}} & \text{for } 0 \le k\Delta x \le \pi \\ -\dfrac{c\cdot\sin k\Delta x}{\sqrt{2(1-\cos k\Delta x)}} & \text{for } -\pi \le k\Delta x \le 0. \end{cases}$$

For $0 \le k\Delta x \le \pi$, the relative error in group velocity is

$$\left| \frac{\omega_1'(k)-c}{c} \right| = \left| \frac{\sin k\Delta x}{\sqrt{2(1-\cos k\Delta x)}} - 1 \right|$$

Similarly, the relative group velocity error for the second integral is

$$\left| \frac{\omega_2'(k)+c}{-c} \right| = \left| \frac{\sin k\Delta x}{\sqrt{2(1-\cos k\Delta x)}} - 1 \right|$$

where $0 \le k\Delta x \le \pi$. The case for $-\pi \le k\Delta x \le 0$ can be analyzed in a similar fashion.

Therefore, the relative group velocity error for $u_j(t)$, which we will abbreviate as E_{gv}, is

$$E_{gv} = \left| \frac{\sin|k|\Delta x}{\sqrt{2(1-\cos k\Delta x)}} - 1 \right| \qquad (4.8)$$

where $-\pi \leq k\Delta x \leq \pi$.

Define N as follows:

$$N = \frac{\text{wavelength of wave with wave number } k}{\text{grid spacing}} = \frac{\lambda}{\Delta x}$$

where $\lambda = \frac{2\pi}{|k|}$. Therefore,

$$N = \frac{2\pi}{|k|\Delta x} .$$

N is the number of grid intervals/ wavelength.

When N = 2, $|k| = \frac{\pi}{\Delta x}$. As $N \to \infty$, $|k| \to 0$. We graph (4.8) as a function of N where N=2,3,4,...,25. See Figure 4.2. For N=2, the superposed waves with wave number $|k|=\frac{\pi}{\Delta x}$ have relative group velocity errors of 1. For N=3 (i.e., $|k|=\frac{2\pi}{3\Delta x}$), the error is about 0.5. Figure 4.3 is the graph of (4.8) with N=6,...,25. Using this graph, we can see that for $N \geq 23$, the curve falls below 1%. This means all waves being superposed to construct $u_j(t)$ that have $|k| \geq \frac{2\pi}{23\Delta x}$ will travel with group velocity within 1% of $\pm c$. The size N has to be for 1% accuracy gives us an intuitive idea of how accurate an approximation scheme (4.1) is.

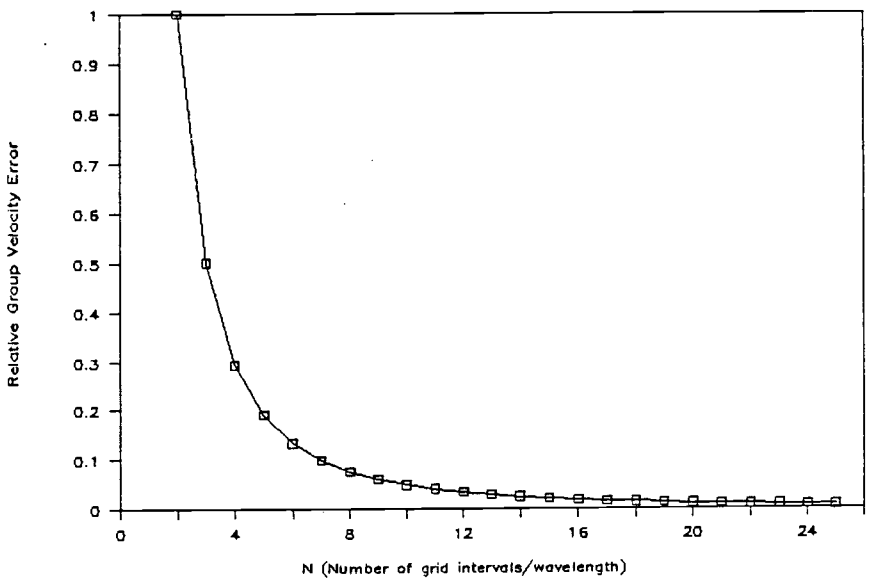

Figure 4.2. E_{gv} for $u_j(t)$, N=2,...,25. The graph of (4.8) as a function N where N=2,...,25.

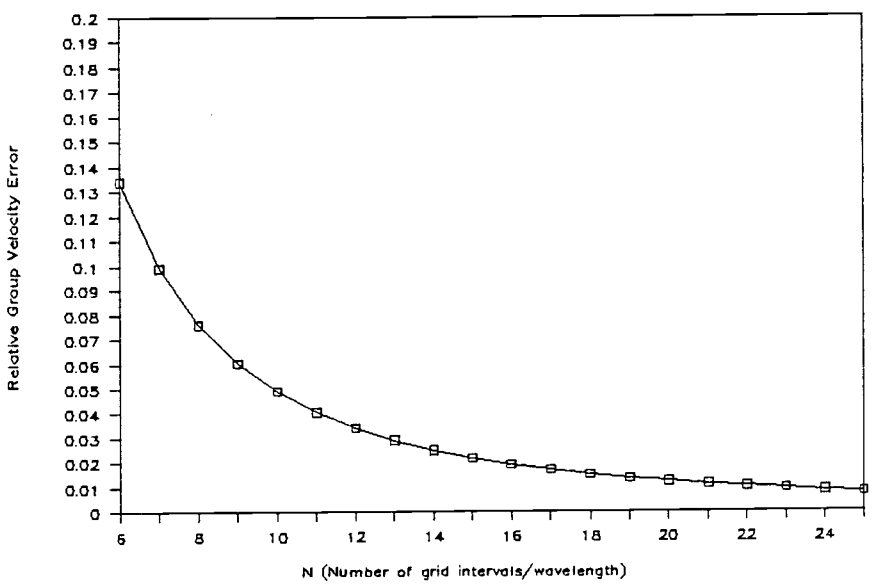

Figure 4.3. E_{gv} for $u_j(t)$, N=6,...,25. The graph of (4.8) as a function of N where N=6,...,25. For $N \geq 23$, the curve drops below the 1% level. This value gives us an

intuitive idea of how accurate an approximation scheme we have and gives us a way of comparing this scheme to those looked at later.

We now obtain our numerical computing scheme from (4.1) using the second order centered finite difference method in time.

Let u_j^n approximate $u_j(n\Delta t)$ for n a positive integer. Define

$$D_t^+ u_j^n = \frac{1}{\Delta t} \cdot (u_j^{n+1} - u_j^n)$$

$$D_t^- u_j^n = \frac{1}{\Delta t} \cdot (u_j^n - u_j^{n-1}).$$

Thus,

$$0 = (\frac{c}{\Delta x})^2 \cdot (u_{j+1}^n - 2 \cdot u_j^n + u_{j-1}^n) - (\frac{1}{\Delta t})^2 \cdot (u_j^{n+1} - 2 \cdot u_j^n + u_j^{n-1}) \quad (4.9)$$

is our numerical computing scheme.

We determine a form for u_j^n . Define

$$\hat{u}_n(k\Delta x) = \Delta x \cdot \sum_{j=-\infty}^{\infty} u_j^n \cdot e^{-i(k\Delta x)j}$$

$$= \sum_{j=-\infty}^{\infty} (\Delta x \cdot u_j^n) \cdot e^{-i(k\Delta x)j} .$$

As before,

$$\Delta x \cdot u_j^n = \frac{1}{2\pi} \cdot \int_{-\pi}^{\pi} \hat{u}_n(k\Delta x) \cdot e^{i(k\Delta x)j} \, d(k\Delta x) .$$

or

$$u_j^n = \frac{1}{2\pi} \cdot \int_{-\pi/\Delta x}^{\pi/\Delta x} \hat{u}_n(k\Delta x) \cdot e^{i(k\Delta x)j}\, dk. \qquad (4.10)$$

To determine a form for $\hat{u}_n(k\Delta x)$, put (4.10) into (4.9), using the same reasoning as before, we get

$$0 = \nu^2 \cdot [e^{ik\Delta x} - 2 + e^{-ik\Delta x}] \cdot \hat{u}_n(k\Delta x) - [\hat{u}_{n+1}(k\Delta x) - 2\hat{u}_n(k\Delta x) + \hat{u}_{n-1}(k\Delta x)] \qquad (4.11)$$

with $\nu = (c\Delta t/\Delta x)$. Thus, we need $\hat{u}(k\Delta x)$ that solves (4.11). Let us assume that (4.11) has a solution of the form

$$A(k) \cdot z^n$$

for some complex function $z = z(k)$. Put this into (4.11) to get

$$z - 2 + z^{-1} = -4\nu^2 \cdot \sin^2 \frac{k\Delta x}{2} . \qquad (4.12)$$

Notice that if z is a solution to (4.12), its inverse z^{-1}, will also be a solution. Therefore, if $A(k) \cdot z^n$ solves (4.11), then so does

$$B(k) \cdot z^{-n} .$$

Thus,

$$\hat{u}_n(k\Delta x) = A(k) \cdot z^n + B(k) \cdot z^{-n}$$

is a general solution to (4.11). So, from (4.10), we get that

$$u_j^n = \frac{1}{2\pi} \int_{-\pi/\Delta x}^{\pi/\Delta x} A(k) \cdot z^n \cdot e^{i(k\Delta x)j}\, dk$$

$$+ \frac{1}{2\pi} \int_{-\pi/\Delta x}^{\pi/\Delta x} B(k) \cdot z^{-n} \cdot e^{i(k\Delta x)j}\, dk. \quad (4.13)$$

is a general solution to (4.9) where z solves (4.12).

Later, it will be shown that:

Claim (1): (4.12) does not have solutions that have both a nonzero imaginary part and absolute value different from 1.

Claim (2): If (4.12) has a solution that is both real and has an absolute value different from 1 then (4.9) will admit solutions that are unstable, a situation we will avoid by requiring $\nu \leq 1$. So, by a simple process of elimination, restricting $\nu \leq 1$ in (4.12) means the only solutions to (4.12) will be complex functions with an absolute value of 1.

For now, let us assume we have shown why claims (1) and (2) are true. Thus, if z is a solution to (4.12), then z has the form

$$z = z(k) = e^{-i\omega\Delta t}$$

for some real $\omega = \omega(k)$. Our problem now is to determine ω. To do so, put (4.13), along with the substitution $z = e^{-i\omega\Delta t}$ into (4.9) to eventually get

$$0 = \nu^2 \cdot (e^{ik\Delta x} - 2 + e^{-ik\Delta x}) - (e^{i\omega\Delta t} - 2 + e^{-i\omega\Delta t}).$$

Solving for ω, we get

$$\omega = \pm \frac{1}{\Delta t} \cos^{-1}(1 - 2\nu^2 \cdot \sin^2 \frac{k\Delta x}{2}).$$

Define ω_1 and ω_2 as follows:

$$\omega_1 = \begin{cases} \frac{1}{\Delta t} \cos^{-1}(1 - 2\nu^2 \cdot \sin^2 \frac{k\Delta x}{2}) & \text{on} \quad 0 \le k\Delta x \le \pi \\ -\frac{1}{\Delta t} \cos^{-1}(1 - 2\nu^2 \cdot \sin \frac{k\Delta x}{2}) & \text{on} \quad -\pi \le k\Delta x \le 0 \end{cases}$$

and $\omega_2 = -\omega_1$.

Therefore,

$$u_j^n = \frac{1}{2\pi} \cdot \int_{-\pi/\Delta x}^{\pi/\Delta x} A(k) \cdot e^{i(k\Delta x)j - i(\omega_1 \Delta t)n} \, dk$$

$$+ \frac{1}{2\pi} \cdot \int_{-\pi/\Delta x}^{\pi/\Delta x} B(k) \cdot e^{i(k\Delta x)j - i(\omega_2 \Delta t)n} \, dk$$

is an integral representation for a general solution to (4.9). We recognize that u_j^n is made up of two travelling waves going in opposite directions. The group velocity error function E_{gv}, for u_j^n will tell us how accurate a numerical computing scheme (4.9) is. We have

$$E_{gv} = \left| \frac{\cos \frac{k\Delta x}{2}}{\sqrt{1 - \nu^2 \cdot \sin^2 \frac{k\Delta x}{2}}} - 1 \right| \qquad (4.14)$$

for $-\pi \le k\Delta x \le \pi$, where we now require $\nu < 1$ to avoid division by zero in (4.14). We call ν the Courant number.

Once again, we can graph (4.14) as a function of N

($k\Delta x = \frac{2\pi}{N}$) for different values of ν. We will study the case with ν=0.5. (Later, when we study the other approximation schemes, their Courant number restrictions will be less than one. We will want to compare numerical approximations from each scheme using a common value for ν. Thus, ν must be chosen small enough so it does not exceed any restrictions). Figure 4.4 is a graph of (4.14) for N=6,...,25, ν= 0.5. In this case, N must be larger than 20 before the superposed waves travel with an error less than 1%. It should be noted that if ν is chosen very close to 1, the curve of (4.14) drops below the 1% at a much smaller value for N. For example, for ν=0.999, (4.14) will be less than 0.01 for N$\geq$3. Thus, as a numerical computing scheme, (4.9) is very accurate for ν close to 1.

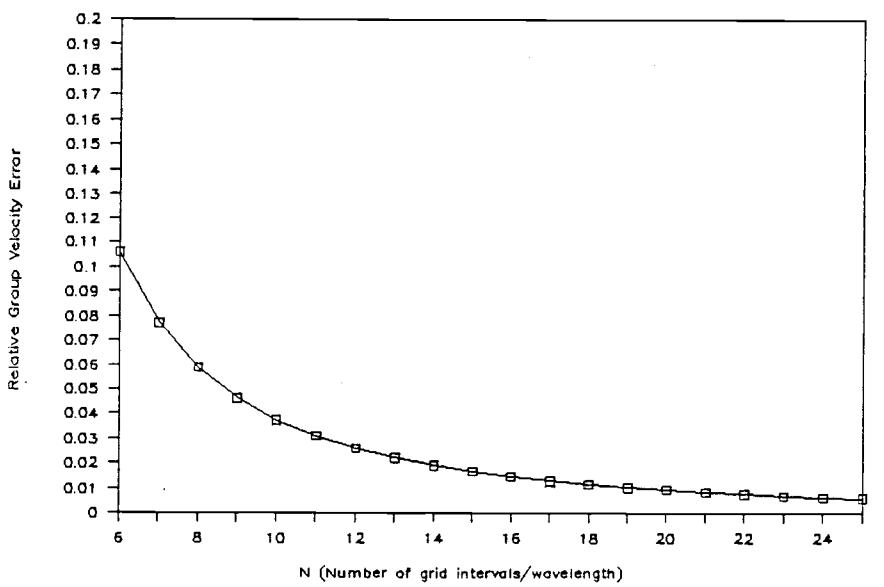

Figure 4.4. E_{gv} for u_j^n, ν=0.5, N=6,...,25. The graph of (4.14) as a function of N where N=6,...,25, ν=0.5. As

the graph indicates, N must be greater than 20 before the curve falls below the 1% level.

We now show why claims (1) and (2) are true.

To show why claim (1) is true, suppose (4.12) had a solution of the form $z = a(k) + ib(k)$ where $|z| \neq 1$ and $b(k) \neq 0$. Choose a k such that $|z(k)| \neq 1$. On a complex plane, we plot $z(k)$ and $z^{-1}(k)$. See Figure 4.5.

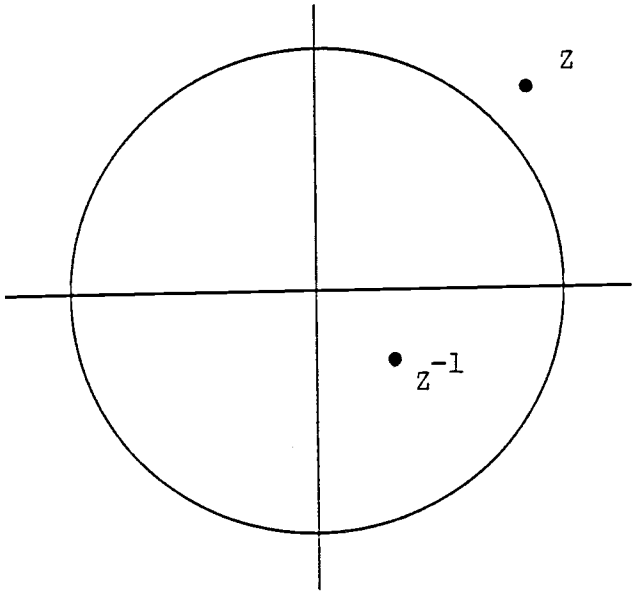

Figure 4.5. The points $z(k)$ and $z^{-1}(k)$ in the complex plane.

Thus, $z(k) - 2 + z^{-1}(k)$ has a nonzero imaginary part. Recall (4.12). We are assuming that z solves (4.12) yet for our chosen k, the left side (4.12) has a nonzero imaginary part while the right side will always be real for any k. Since this leads us to a contradiction, we conclude that

(4.12) cannot have a solution that has both a nonzero imaginary part and absolute value different from 1.

For claim (2), suppose that z was a solution to (4.12) where z was both real and with absolute value different from 1. From (4.12), we can determine a form for z by using the quadratic formula.

We get

$$z = 1 - 2\nu^2 \cdot \sin^2\frac{k\Delta x}{2} \pm 4\nu \cdot \sin\frac{k\Delta x}{2} \cdot \sqrt{\nu^2 \cdot \sin^2\frac{k\Delta x}{2} - 1} \quad .$$

From this form for z, we see that z is a continuous real function. We are assuming that the norm of z is not equal to 1, so there exists k_0 such that $|z(k_0)| \neq 1$. We assume that $|z(k_0)| > 1$ (if $|z(k_0)| < 1$, then replace z with z^{-1}). By the continuity of z, there exists α and β such that $z > 1$ on (α, β). Consider

$$\frac{1}{2\pi} \cdot \int_{\alpha}^{\beta} z^n \cdot e^{i(k\Delta x)l} \, dk. \qquad (4.15)$$

This is a solution to (4.9) (perhaps, think of this integral as a solution to (4.9) for some particular IVP). Imagine (4.15) as a superposition of waves where each wave has an amplitude $|z^n| \to \infty$ as $n \to \infty$. This means (4.15) is a travelling wave that has an amplitude increasing to infinity as time goes on. Thus, (4.15) is an unstable solution to (4.9), something we do not want to allow. We will avoid this problem by not allowing (4.12) to have real solutions with absolute value different from one. This can be en-

sured by restricting $\nu \leq 1$. To see why this is a sufficient restriction, consider an arbitrary real function z with $|z| \neq 1$. For any value of k, $z - 2 + z^{-1}$ will be a real number in $(-\infty, -4) \cup (0, \infty)$. We can see this by drawing the graph of $f(z) = z - 2 + z^{-1}$ for z real. See Figure 4.6.

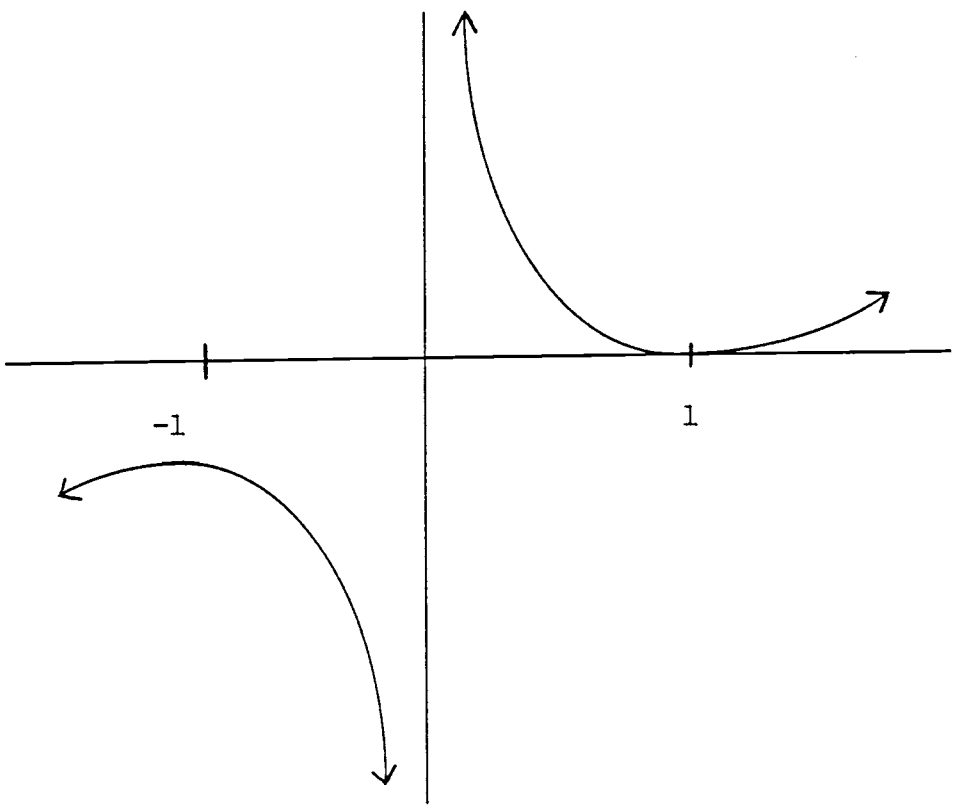

Figure 4.6. The graph of $f(z) = z - 2 + z^{-1}$ for z real.

Therefore, to ensure that z will not solve (4.12), we will bound ν such that

$$-4 \leq -4\nu^2 \cdot \sin^2 \frac{k\Delta x}{2} \leq 0 \ ,$$

i.e., $\nu \leq 1$.

Consider the test problem

$$u_{tt} = u_{xx}$$

$$u(x,0) = e^{-500(x-0.5)^2}$$

$$u_t(x,0) = 0$$

$$u(0,t) = u(4,t) = 0$$

for $0 \leq x \leq 4$, $t > 0$. We will determine numerical solutions for this problem using (4.9). Since c=1, (4.9) becomes

$$u_j^{n+1} = (\frac{\Delta t}{\Delta x})^2 \cdot (u_{j+1}^n - 2u_j^n + u_{j-1}^n) + (2u_j^n - u_j^{n-1}) .$$

We let $\Delta x = 0.02$ and $\Delta t = 0.01$, thus $\nu = 0.5$. Because of the given initial and boundary conditions, we choose

$$u_j^0 = e^{-500(j\cdot\Delta x-0.5)^2}$$
$$u_0^n = u_{200}^n = 0.$$

Our numerical scheme will not give values for u_j^1, so instead we will use Taylor's Theorem to estimate u_j^1. For u the solution to our test problem, fix x and consider

$$u(x,\Delta t) = u(x,0) + u_t(x,0)\cdot\Delta t + u_{tt}(x,\eta)\cdot\frac{\Delta t^2}{2}$$

for some η between 0 and Δt. Since $u_t(x,0) = 0$,

$$u(x,\Delta t) = u(x,0) + 0(\Delta t)^2.$$

Thus, we let

$$u_j^1 = e^{-500(j\cdot\Delta x-0.5)^2}.$$

Figure 4.7 is a graph of the approximations for n=199. In the exact solution to the wave equation, we would see two pulses centered at $x=\frac{5}{2}$ and $x=\frac{3}{2}$, each of height 0.5 (the pulse at $x=\frac{3}{2}$ is the result of reflection at $x=0$ and the negative reflection is due to the Direchlet boundary condition). In the numerical solution, we see two pulses with heights a little less than 0.5. Neither of the pulses are exactly at the points $x=\frac{5}{2}$ and $x=\frac{3}{2}$ and shorter waves trail behind each of them. This illustrates the idea of dispersion.

It should be noted that in a more realistic setting, we would not have picked Δx so large in comparison to the width of the pulse at t=0. (For this Δx, the pulse at t=0 is about 18 grid intervals wide. This is determined by looking at a computer printout of the values of the pulse when t=0 and rounding each value to six decimal places.) We picked Δx as above so that dispersion will occur as quickly as possible.

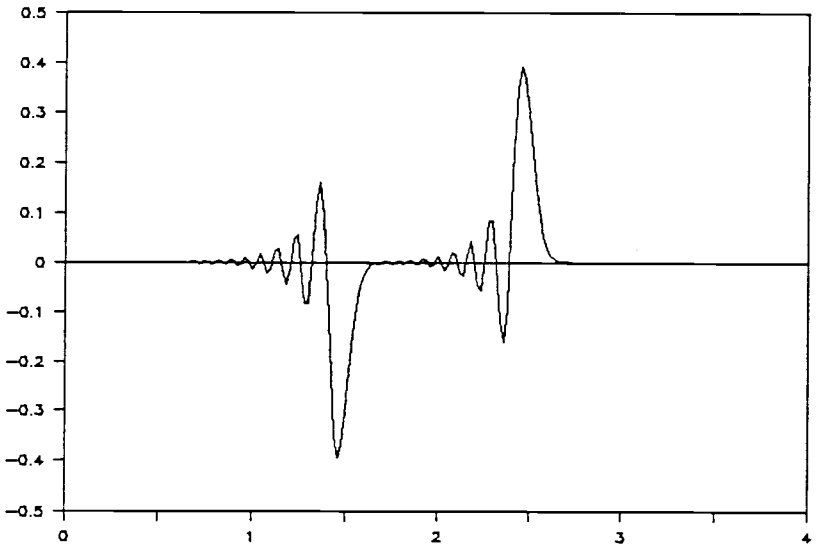

Figure 4.7. Test problem for u_j^n, ν=0.5. The graph of (4.9) for the test problem where ν=0.5, n=199. Dispersion is occurrng at both pulses. Higher wave number have lower group velocities and so these waves lag behind the main pulse.

5. THE LINEAR FINITE ELEMENT METHOD IN 1-D

The next method we will use to approximate the spatial derivative in the wave equation is the linear finite element method.

Some general references on the finite element methods are [Fletcher], [Strang and Fix], and [Lapidus and Pinder].

Define

$$\mathcal{L}[u] = c^2 \cdot u_{xx} - u_{tt}.$$

We want to solve

$$\mathcal{L}[u] = 0$$

for $0 < x < L$, $t > 0$ with initial conditions

$$u(x,0) = f(x)$$

$$u_t(x,0) = g(x).$$

For convenience, we will consider the boundary conditions

$$u(0,t) = 0$$

$$u(L,t) = 0$$

for $t > 0$.

If $\mathcal{L}[u] = 0$, then

$$0 = \int_0^L \mathcal{L}[u] \cdot w(x)\, dx$$

for any function $w(x)$. If $w \in C^1[0,L]$, then

$$0 = \int_0^L (c^2 \cdot u_{xx} - u_{tt}) \cdot w(x)\, dx$$

$$= c^2 \cdot u_x(L,t) \cdot w(L) - c^2 \cdot u_x(0,t) \cdot w(0)$$

$$- c^2 \cdot \int_0^L u_x \cdot \frac{d}{dx} w\, dx - \int_0^L u_{tt} \cdot w\, dx. \quad (5.1)$$

If (5.1) is satisfied for all $w \in C^1[0,L]$, then we can reverse the above argument to show that $\mathcal{L}[u] = 0$ (provided that u_{xx} exists). We call (5.1) the weak form of the partial differential equation $\mathcal{L}[u] = 0$.

Divide $[0,L]$ into R equal parts of size Δx, and suppose that we approximate u with the piecewise linear function

$$\hat{u}(x,t) = \sum_{r=0}^{R} u_r(t) \cdot \phi_r(x),$$

where $\{\phi_r\}$ is the linear finite element basis defined by

$$\phi_0(x) = \begin{cases} 1 - \frac{x}{\Delta x}, & 0 \le x \le x_1 \\ 0, & x \ge x_1 \end{cases}$$

$$\phi_r(x) = \begin{cases} \frac{x - x_{r-1}}{\Delta x}, & x_{r-1} \le x \le x_r \\ 1 - \frac{x - x_r}{\Delta x}, & x_r \le x \le x_{r+1} \\ 0, & \text{otherwise} \end{cases}$$

$$\phi_R(x) = \begin{cases} 0, & 0 \le x \le x_{R-1} \\ \frac{x - x_{R-1}}{\Delta x}, & x_{R-1} \le x \le x_R. \end{cases}$$

Figures 5.1 and 5.2 are the graphs of these basis elements.

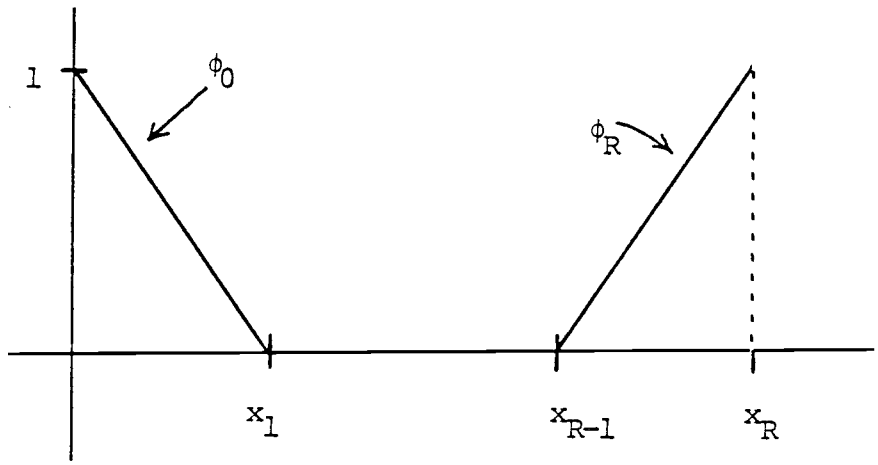

Figure 5.1. The graphs of ϕ_0 and ϕ_R. These two are the linear finite element bases located at the boundaries of $[0,L]$.

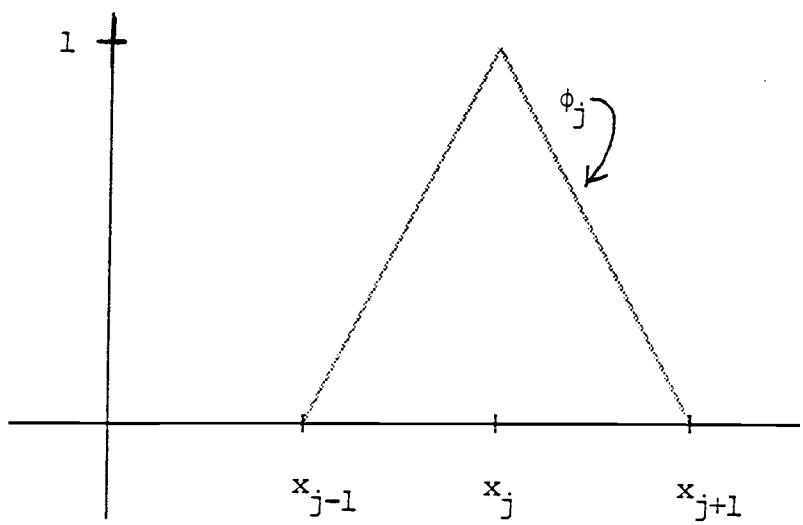

Figure 5.2. The graph of ϕ_j where $1 \leq j \leq R-1$. These bases appear throughout $[0,L]$ where ϕ_j is centered at x_j.

We will set $u_0(t)$ and $u_R(t)$ equal to zero, so that $\sum u_r(t)\cdot\phi_r(x)$ is zero at $x=0$ and $x=L$, in agreement with the boundary conditions. For different boundary conditions, $u_0(t)$ and $u_R(t)$ might be nonzero. Therefore, we are approximating u by

$$\hat{u}(x,t) = \sum_{r=1}^{R-1} u_r(t)\cdot\phi_r(x).$$

We will replace u with $\hat{u}$ in (5.1) and try to determine a form for $u_r(t)$. This poses a problem for us because (5.1) will require $\frac{\partial}{\partial x}\hat{u}$ to exist for all x in [0,L], i.e., for $\frac{d}{dx}\phi_r$ to exist for all x in [0,L], r=1,...,R-1. Since ϕ_r has corners at x_{r-1}, x_r, and x_{r+1}, $\frac{d}{dx}\phi_r$ will not exist there. It turns out that this dilemma will not affect our analysis in any way. Therefore, we will simply proceed forwards. In (5.1), replace u with the summand representation for $\hat{u}$. We then obtain an equation with R−1 unknowns, these unknowns being $u_r(t)$, $1 \le r \le R-1$. Define w(x) as $\phi_j(x)$ for $1 \le j \le R-1$ and obtain a system of R−1 equations with R−1 unknowns. Thus, (5.1) yields

$$0 = c^2\cdot\left[\sum_{r=1}^{R-1} u_r(t)\cdot\frac{d}{dx}\phi_r(L)\right]\cdot\phi_j(L) - c^2\cdot\left[\sum_{r=1}^{R-1} u_r(t)\cdot\frac{d}{dx}\phi_r(0)\right]\cdot\phi_j(0)$$

$$- c^2\cdot\sum_{r=1}^{R-1} u_r(t)\cdot\int_0^L \frac{d}{dx}\phi_r\cdot\frac{d}{dx}\phi_j\,dx - \sum_{r=1}^{R-1} u_r''(t)\cdot\int_0^L \phi_r\cdot\phi_j\,dx \qquad (5.2)$$

for $1 \le j \le R-1$, with

$$\frac{d}{dx}\phi_j = \begin{cases} \frac{1}{\Delta x} & \text{for } x_{j-1} < x < x_j \\ -\frac{1}{\Delta x} & \text{for } x_j < x < x_{j+1}. \\ \text{undefined at } x_{j-1}, x_j, \text{ and } x_{j+1} \\ 0 \quad \text{elsewhere.} \end{cases}$$

This is called the distribution derivative of ϕ_j.

Since $\phi_j(L) = \phi_j(0) = 0$ if $1 \leq j \leq R-1$, the first two terms of (5.2) are zero. Equation (5.2) reduces to

$$0 = c^2 \cdot \sum_{r=1}^{R-1} u_r(t) \cdot \int_0^L \frac{d}{dx}\phi_r \cdot \frac{d}{dx}\phi_j \, dx + \sum_{r=1}^{R-1} u_r''(t) \cdot \int_0^L \phi_r \cdot \phi_j \, dx. \qquad (5.3)$$

By considering the size of the support for each basis element, (5.3) becomes

$$0 = c^2 \cdot [\, u_{j-1}(t) \cdot \int_0^L \phi_{j-1}' \cdot \phi_j' \, dx + u_j(t) \cdot \int_0^L (\phi_j')^2 \, dx + u_{j+1}(t) \cdot \int_0^L \phi_j' \cdot \phi_{j+1}' dx \,]$$

$$+ [\, u_{j-1}''(t) \cdot \int_0^L \phi_{j-1} \cdot \phi_j \, dx + u_j''(t) \cdot \int_0^L (\phi_j)^2 \, dx + u_{j+1}''(t) \cdot \int_0^L \phi_j \cdot \phi_{j+1} \, dx \,]$$

for $j = 1, \ldots, (R-1)$.

We evaluate a few integrals.

Consider $\int_0^L \phi_j \cdot \phi_{j+1} \, dx$. Figure 5.3 is a drawing of ϕ_j and ϕ_{j+1}.

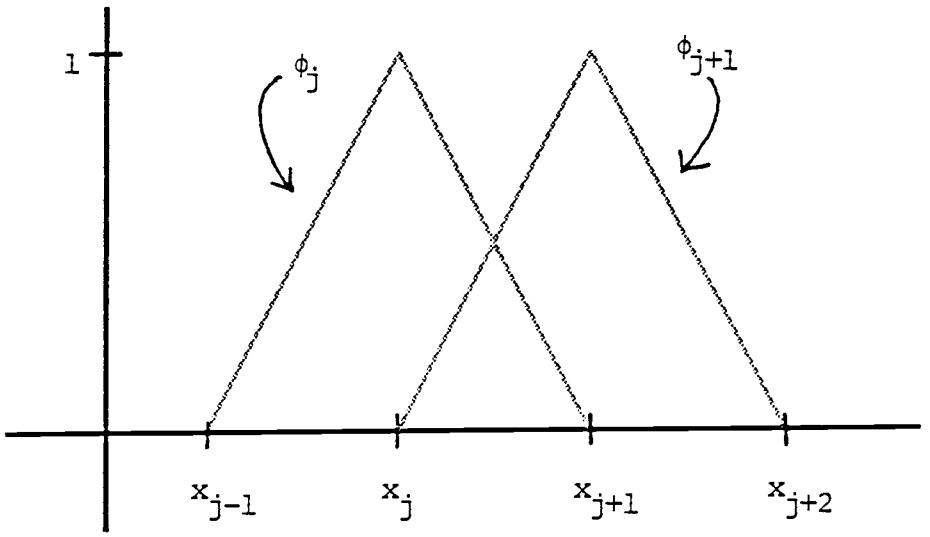

Figure 5.3. The graphs of ϕ_j and ϕ_{j+1} for $1 \leq j \leq (R-1)$.

Relabel ϕ_j and ϕ_{j+1} as ϕ_0 and ϕ_1, respectively and relocate them both towards the origin by translating x_j to 0. Thus,

$$\begin{aligned}
\int_0^L \phi_j \cdot \phi_{j+1}\, dx &= \int_0^{\Delta x} \phi_0 \cdot \phi_1\, dx \\
&= \int_0^{\Delta x} (1 - \tfrac{x}{\Delta x}) \cdot (\tfrac{x}{\Delta x})\, dx \\
&= \Delta x \cdot \int_0^1 (1 - \xi) \cdot \xi\, dx, \quad \xi = \tfrac{x}{\Delta x} \\
&= \tfrac{\Delta x}{6} .
\end{aligned}$$

Next, we evaluate $\int_0^L \phi_j^2(x)\, dx$. Recall Figure 5.2. Relabel ϕ_j as ϕ_0 and relocate this towards the origin by translating x_j to 0. Thus,

$$\int_0^L \phi_j^2(x)\ dx = 2\cdot\int_0^{\Delta x} (1 - \tfrac{x}{\Delta x})^2\ dx$$

$$= \tfrac{2}{3}\cdot\Delta x\ .$$

In similar fashion, we evaluate the following:

$$\int_0^L \tfrac{d\phi_j}{dx}\cdot\tfrac{d\phi_{j+1}}{dx}\ dx = \int_0^{\Delta x} \tfrac{d\phi_0}{dx}\cdot\tfrac{d\phi_1}{dx}\ dx$$

$$= \int_0^{\Delta x} (-\tfrac{1}{\Delta x})\cdot(\tfrac{1}{\Delta x})\ dx$$

$$= -\tfrac{1}{\Delta x}$$

and

$$\int_0^L \tfrac{d\phi_j}{dx}\cdot\tfrac{d\phi_j}{dx}\ dx = 2\cdot\int_0^{\Delta x} (\tfrac{1}{\Delta x})^2\ dx$$

$$= \tfrac{2}{\Delta x}\ .$$

Evaluation of the remaining integrals is obtained by symmetry. Substitution and simplification gives

$$0 = \tfrac{c^2}{\Delta x^2}\cdot\ (\ u_{j-1}(t) - 2\cdot u_j(t) + u_{j+1}(t)\ )$$

$$- \ (\ \tfrac{1}{6}\cdot u''_{j-1}(t) + \tfrac{2}{3}\cdot u''_j(t) + \tfrac{1}{6}\cdot u''_{j+1}(t)\ )\ .\quad (5.4)$$

We call this equation the linear finite element approximation scheme. Compare (5.4) to (4.1). The second term of (5.4) contains a weighted average of $u''_j(t)$ whereas the second term of (4.1) is just $u''_j(t)$.

Proceeding as before, we end up with a group velocity equation,

$$E_{gv} = \left|\tfrac{9}{\sqrt{6}}\cdot\ \frac{\sin|k|\Delta x}{(2+\cos k\Delta x)^{3/2}}\cdot\ \frac{1}{(1-\cos k\Delta x)^{1/2}} - 1\right| \qquad (5.5)$$

for $-\pi \leq k\Delta x \leq \pi$.

Figure 5.4 is the graph of (5.5) for N=6,...,25. Compare this graph to that of (4.8). There is very little difference between them. This means that approximating the spatial derivative in the wave equation with the linear finite element method is comparable to using the second order centered finite difference method.

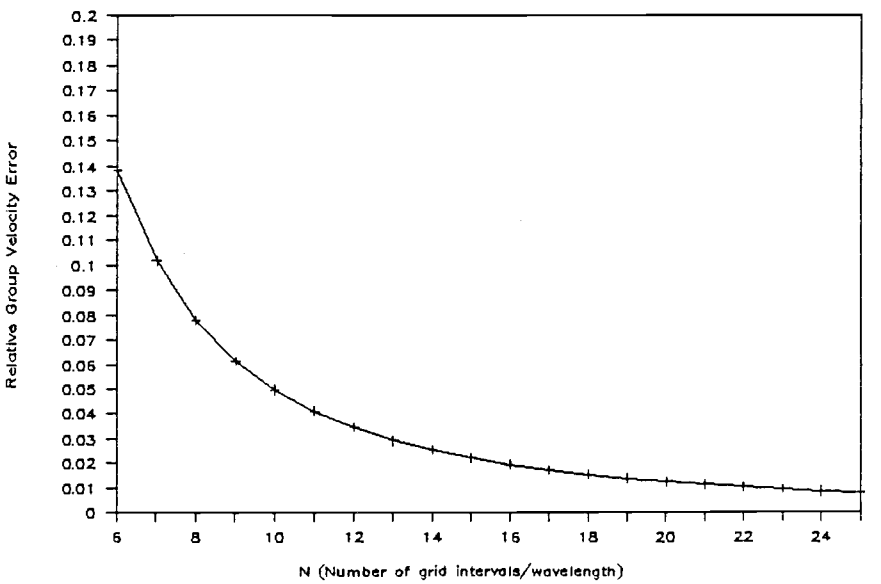

Figure 5.4. E_{gv} for $u_j(t)$, N=6,...,25. The graph of (5.5) as a function of N where N=6,...,25. There is little difference between this graph and the graph for (4.8).

We now obtain a numerical computing scheme from (5.4)

by replacing $u_r''(t)$ with $\frac{1}{\Delta t}\cdot (u_r^{n+1} - 2\cdot u_r^n + u_r^{n-1})$ for r = j−1, j, and j+1. Thus, we get

$$0 = \nu^2\cdot(u_{j+1}^n - 2\cdot u_j^n + u_{j-1}^n) - \frac{1}{6}\cdot (u_{j+1}^{n+1} - 2\cdot u_{j+1}^n + u_{j+1}^{n-1})$$

$$- \frac{2}{3}\cdot(u_j^{n+1} - 2\cdot u_j^n + u_j^{n-1}) - \frac{1}{6}\cdot(u_{j-1}^{n+1} - 2\cdot u_{j-1}^n + u_{j-1}^{n-1}), \quad (5.6)$$

where $\nu = c\Delta t/\Delta x$.

We are interested in obtaining E_{gv} from (5.6). We proceed as before to get (after much manipulation)

$$(2 + \cos k\Delta x)z - 4 + (2+ \cos k\Delta x)z^{-1} =$$

$$-12\cdot\nu^2\cdot\sin^2\frac{k\Delta x}{2} + 2\cdot\cos k\Delta x. \quad (5.7)$$

As in section 4, we need a restriction on ν so that (5.7) does not admit real solutions with an absolute value different from one. Assume z is real and define

$$f(z) = (2 + \cos k\Delta x)z - 4 + (2 + \cos k\Delta x) z^{-1} .$$

We find the range of f. Since

$$f'(z) = (2 + \cos k\Delta x) - (2 + \cos k\Delta x)z^{-2},$$

we have that $f'(z) = 0$ if $z=1,-1$. Thus, f has a local min of

$$2 (2 + \cos k\Delta x) - 4 \qquad \text{at} \quad z=1$$

and a local max of

$$-2 (2 + \cos k\Delta x) - 4 \qquad \text{at} \quad z=-1.$$

Figure 5.5 is a general sketch of its graph.

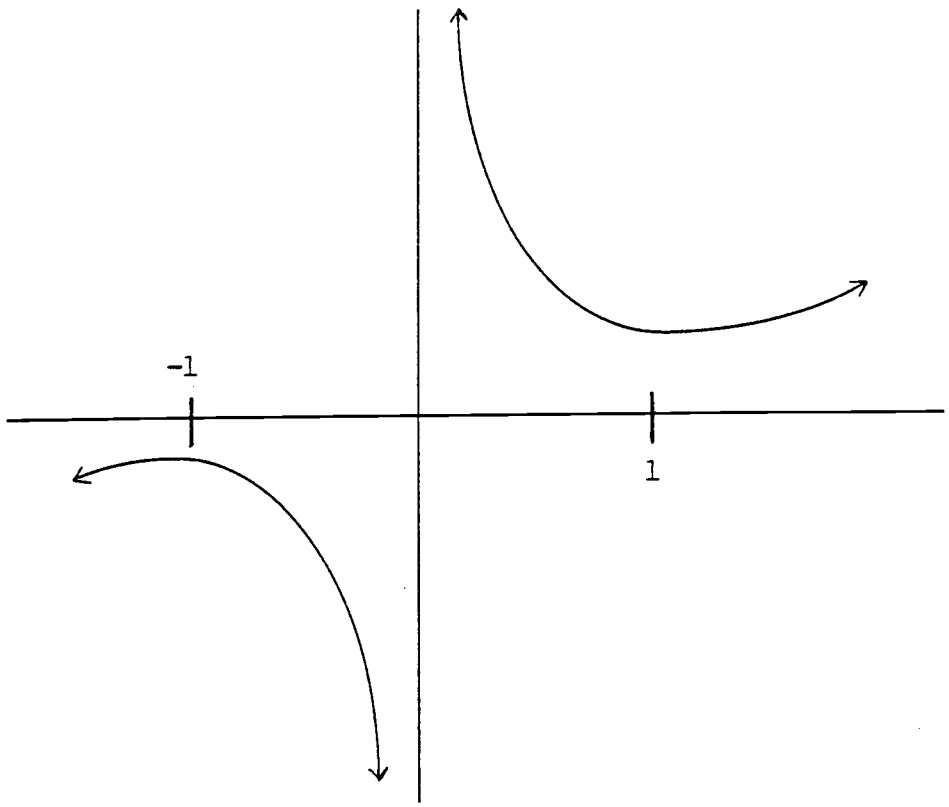

Figure 5.5. Sketch of $f(z) = (2+\cos k\Delta x)z - 4 + (2 + \cos k\Delta x)z^{-1}$. Here, z is real and $k\Delta x$ is fixed.

Thus, the range of f is

$$(-\infty\ ,\ -2\cdot\ [2 + \cos k\Delta x]\ -\ 4\ ]$$
$$\cup\ [\ 2\cdot\ [2 + \cos k\Delta x]\ -\ 4\ \ ,\ \infty\ )\ .$$

Like before, we want to determine a bound on ν such that

$$-2\cdot\ [2 + \cos k\Delta x]\ -\ 4\ \leq\ \ -12\cdot\ \nu^2\cdot\ \sin^2\frac{k\Delta x}{2}\ +\ 2\cdot\ \cos k\Delta x$$
$$\leq\ \ 2\cdot\ [2 + \cos k\Delta x]\ -\ 4 \qquad (5.8)$$

for all values of $k\Delta x$. We break up (5.8) into two parts.

The first inequality of (5.8) yields

$$\nu^2 \leq \frac{8 + 4\cdot\cos k\Delta x}{12\cdot\sin^2\frac{k\Delta x}{2}}.$$

This holds true for all $k\Delta x$ if we require $\nu \leq \frac{\sqrt{3}}{3}$. The second inequality of (5.8) yields $\nu \geq 0$, which is always true by definition of ν. Thus, we require that $\nu \leq \frac{\sqrt{3}}{3}$.

If we proceed as before, we eventually will end with

$$E_{gv} = \left| \frac{6\cdot[(2 + \cos k\Delta x)\cdot(\cos\frac{k\Delta x}{2}) + (\sin\frac{|k|\Delta x}{2})\cdot(\sin|k|\Delta x)]}{(2 + \cos k\Delta x)\cdot\sqrt{12\cdot(2 + \cos k\Delta x) - 36\cdot\nu^2\cdot\sin^2\frac{k\Delta x}{2}}} - 1 \right| \tag{5.9}$$

where, in addition, we require $\nu < \frac{\sqrt{3}}{3}$ to avoid division by zero.

The graph of (5.9) as a function of N where N=6, . . . ,25 and ν=0.5 is given in Figure 5.6. We will need N≥26 for the relative velocity error to drop below 1%. Thus, as a numerical computing scheme, (5.6) is very comparable to (4.9) for the reasonable ν=0.5. The difference between (4.9) and (5.6) is that (4.9) is an explicit scheme and easy to program into a computer while (5.6) is an implicit scheme and programming it will require us to convert it into a tridiagonal matrix equation first.

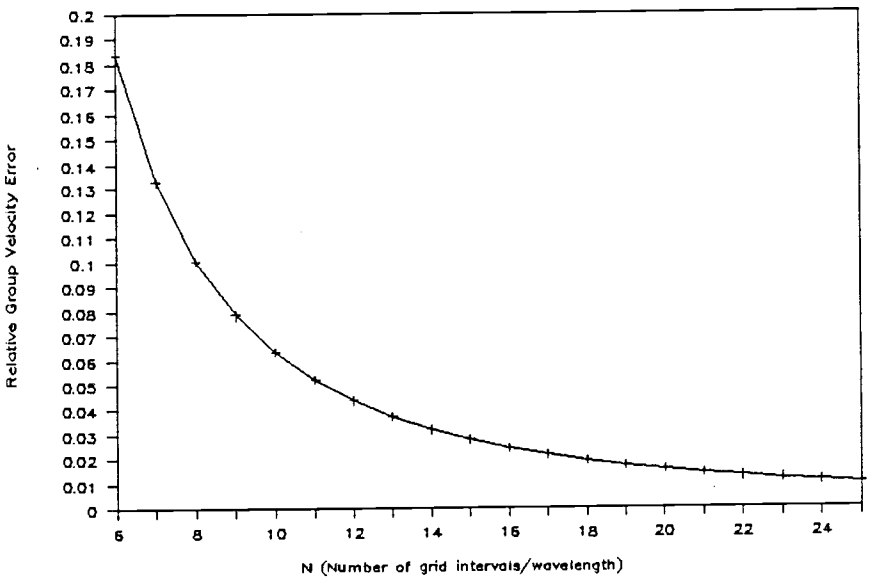

Figure 5.6. E_{gv} for u_j^n, $\nu=0.5$, $N=6,\ldots,25$. The graph of (5.9) as a function of N where $N=6,\ldots,25$ with $\nu=0.5$. For $N\geq 26$, the curve drops below the 1% level. On this fact, we can predict that the numerical computing schemes (5.6) and (4.9) will give comparable results.

To use (5.6) for our test problem from section 4, we will have to solve the matrix equation $A\hat{x}=\hat{b}$ where A is a 199 x 199 tridiagonal $(\frac{1}{6},\frac{2}{3},\frac{1}{6})$ matrix, $\hat{x}$ is the vector of numerical approximations at time level n and $\hat{b}$ is a vector we obtain by using the numerical values from previous time levels. Figure 5.7 is a graph of the approximations for $\nu=0.5$ and $t=2$. It looks quite similar to Figure 4.6. As predicted, the amount of dispersion that has occurred here

is about the same as the amount we saw in section 4. In the case of Figure 5.7, the dispersion leads the main pulses whereas the dispersion in Figure 4.7 follows the main pulses. What is probably happening is that the higher wave numbers have higher group velocities. Consider the solution u_j^n to (5.6). The superposing waves that have wave numbers with a large magnitude are travelling with a group speed slightly greater than $|c|$.

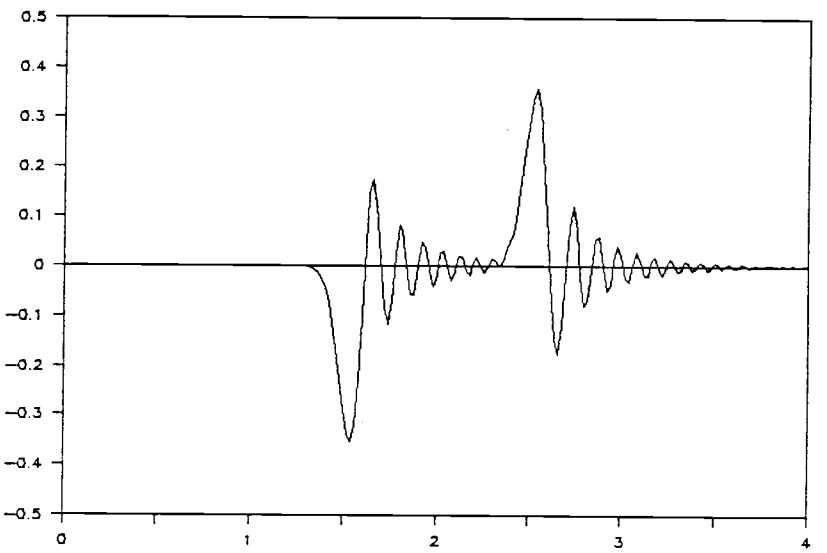

Figure 5.7. Test problem for u_j^n, $\nu=0.5$. The graph of (5.6) for the test problem where $\nu=0.5$, $n=199$. The amount of dispersion occurring is similar to that found in Figure 4.7. In the case of Figure 5.7, the dispersion leads the main pulses whereas the dispersion in Figure 4.7 follows the main pulses.

6. THE QUADRATIC FINITE ELEMENT METHOD IN 1-D

The next method we look at to approximate the spatial derivative in the wave equation is called the quadratic finite element method. To implement this method, we replace the linear basis from section 5 with a new basis called the quadratic basis which we will still label as $\{\phi_r\}$. The elements of this set are

$$\phi_0(x) = \begin{cases} -\frac{1}{2}\cdot\frac{x-\Delta x}{\Delta x} + \frac{1}{2}\cdot\left[\frac{x-\Delta x}{\Delta x}\right]^2 & \text{for } 0 \le x \le x_2 \\ 0 & \text{otherwise} \end{cases}$$

$$\phi_r(x) = \begin{cases} 1 - \left[\frac{x-x_r}{\Delta x}\right]^2 & \text{for } x_{r-1} \le x \le x_{r+1} \quad (r \text{ odd}) \\ 0 & \text{otherwise} \end{cases}$$

$$\phi_r(x) = \begin{cases} \frac{1}{2}\cdot\left[\frac{x-x_{r-1}}{\Delta x}\right] + \frac{1}{2}\cdot\left[\frac{x-x_{r-1}}{\Delta x}\right]^2 & \text{for } x_{r-2} \le x \le x_r \ (r \text{ even}) \\ -\frac{1}{2}\cdot\left[\frac{x-x_{r+1}}{\Delta x}\right] + \frac{1}{2}\cdot\left[\frac{x-x_{r+1}}{\Delta x}\right]^2 & \text{for } x_r \le x \le x_{r+1} \\ 0 & \text{otherwise} \end{cases}$$

$$\phi_R(x) = \begin{cases} \frac{1}{2}\cdot\left[\frac{x-x_{R-1}}{\Delta x}\right] + \frac{1}{2}\cdot\left[\frac{x-x_{R-1}}{\Delta x}\right]^2 & \text{for } x_{R-2} \le x \le x_R \\ 0 & \text{elsewhere} \end{cases}$$

where R is chosen to be even. Notice that for r odd, ϕ_r has support $[x_{r-1}, x_{r+1}]$ and for r even, ϕ_r has support $[x_{r-2}, x_{r+2}]$. We will present the graphs of the ϕ_r's later on in this section.

For our new definition of ϕ_r, consider the function $\hat{u} = \sum u_r(t) \cdot \phi_r(x)$ where $\hat{u}$ is the function we will use to approximate u. For t fixed, $\hat{u}$ is a linear combination of the ϕ_r's. Since each ϕ_r is quadratic and continuous, $\hat{u}$ is a continuous piecewise quadratic function on $[0, L]$. We will show that on any interval of the form $[x_{r-1}, x_{r+1}]$ with r odd, every quadratic polynomial on that interval is a linear combination of ϕ_{r-1}, ϕ_r, and ϕ_{r+1}. Thus, if $[0, L]$ is divided into an even number of subintervals, then every continuous piecewise quadratic function on $[0, L]$ can be written as a linear combination of $\phi_0, \ldots, \phi_R$. By defining $\hat{u}$ as we do, we are thus considering all continuous piecewise quadratic functions on our given grid of $[0, L]$ for our analysis.

Let f be some quadratic function defined on $[x_{r-1}, x_{r+1}]$. We will show that f can be written as a linear combination of ϕ_{r-1}, ϕ_r, and ϕ_{r+1}. In other words, we will find constants α, β, and γ such that

$$f(x) = \alpha \cdot \phi_{r-1}(x) + \beta \cdot \phi_r(x) + \gamma \cdot \phi_{r+1}(x)$$

for all $x \in [x_{r-1}, x_{r+1}]$. Define $\alpha = f(x_{r-1})$, $\beta = f(x_r)$, and

$\gamma = f(x_{r+1})$. By the definition of ϕ_r, it is equal to one at x_r and zero at all other gridpoints. So, $\alpha\cdot\phi_{r-1} + \beta\cdot\phi_r + \gamma\cdot\phi_{r+1}$ is equal to f for $x = x_{r-1}$, x_r, and x_{r+1}. At this point, we will claim that $\alpha\cdot\phi_{r-1} + \beta\cdot\phi_r + \gamma\cdot\phi_{r+1}$ and f are equal to each other for all $x \in [x_{r-1}, x_{r+1}]$. To see why this is so, define

$$g(x) = f(x) - \alpha\cdot\phi_{r-1}(x) + \beta\cdot\phi_r(x) + \gamma\cdot\phi_{r+1}(x).$$

We have that g is either a quadratic, linear, or constant function on the interval $[x_{r-1}, x_{r+1}]$. We know that g has at least three roots, viz., at $x = x_{r-1}$, x_r, and x_{r+1}. Since neither a quadratic, linear, nor nonzero constant function can have three roots, we conclude that $g(x)$ is the zero function. Thus, our claim is proven and we conclude that

$$f(x) = \alpha\cdot\phi_{r-1}(x) + \beta\cdot\phi_r(x) + \gamma\cdot\phi_{r+1}(x)$$

for all $x \in [x_{r-1}, x_{r+1}]$ with α, β, and γ defined as above.

From our previous work, we have

$$0 = c^2\cdot \sum_{r=1}^{R-1} u_r(t)\cdot \int_0^L \phi_r'\cdot \phi_j'\, dx + \sum_{r=1}^{R-1} u_r''(t)\cdot \int_0^L \phi_r\cdot\phi_j\, dx$$

where in this case, the length of the support for ϕ_j depends on whether j is either odd or even. For j odd, we have

$$0 = c^2\cdot \{ u_{j-1}(t)\cdot \int_0^L \phi_{j-1}'\cdot\phi_j'\, dx + u_j(t)\cdot \int_0^L \phi_j'^{\,2}\, dx + u_{j+1}(t)\cdot \int_0^L \phi_{j+1}'\cdot\phi_j'\, dx \}$$

$$+ \{ u''_{j-1}(t)\cdot\int_0^L \phi_{j-1}\cdot\phi_j\,dx + u''_j(t)\cdot\int_0^L \phi_j^2\,dx + u''_{j+1}(t)\cdot\int_0^L \phi_{j+1}\cdot\phi_j\,dx \} \qquad (6.1)$$

and for j even

$$0 = c^2\cdot \{ u_{j-2}(t)\cdot\int_0^L \phi'_{j-2}\cdot\phi'_j\,dx + u_{j-1}(t)\cdot\int_0^L \phi'_{j-1}\cdot\phi_j'\,dx + u_j(t)\cdot\int_0^L \phi_j'^{\,2}\,dx$$
$$+ u_{j+1}(t)\cdot\int_0^L \phi'_{j+1}\cdot\phi'_j\,dx + u_{j+2}(t)\cdot\int_0^L \phi'_{j+2}\cdot\phi'_j\,dx \}$$
$$+ \{ u''_{j-2}(t)\cdot\int_0^L \phi_{j-2}\cdot\phi_j\,dx + u''_{j-1}(t)\cdot\int_0^L \phi_{j-1}\cdot\phi_j\,dx + u''_j(t)\cdot\int_0^L \phi_j^2\,dx$$
$$+ u''_{j+1}(t)\cdot\int_0^L \phi_{j+1}\cdot\phi_j\,dx + u''_{j+2}(t)\cdot\int_0^L \phi_{j+2}\cdot\phi_j\,dx \}. \qquad (6.2)$$

Each integral from (6.1) and (6.2) must be evaluated. Consider the integrals in (6.1). Figure 6.1 contains graphs of ϕ_{j-1}, ϕ_j, and ϕ_{j+1} over the support of ϕ_j where j odd.

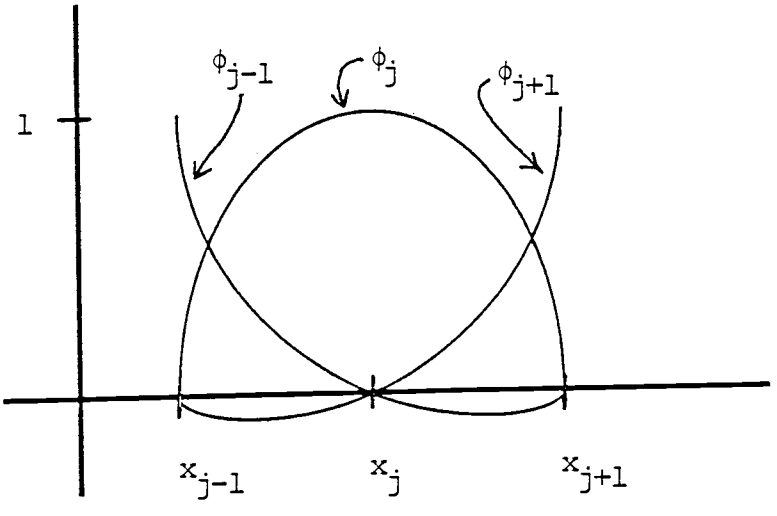

Figure 6.1. The graphs of ϕ_{j-1}, ϕ_j, and ϕ_{j+1}, j odd. This is graphed over the support of ϕ_j.

We can integrate easily if we relocate these towards the origin such that ϕ_j is centered at the origin. We relabel them as ϕ_L , ϕ_C , and ϕ_R where

$$\phi_C(x) = 1 - (\tfrac{x}{\Delta x})^2$$

$$\phi_L(x) = -\tfrac{1}{2}\cdot\tfrac{x}{\Delta x} + \tfrac{1}{2}\cdot(\tfrac{x}{\Delta x})^2$$

$$\phi_R(x) = \tfrac{1}{2}\cdot\tfrac{x}{\Delta x} + \tfrac{1}{2}\cdot(\tfrac{x}{\Delta x})^2$$

on $-\Delta x \le x \le \Delta x$. Thus, for (6.1),

$$\int_0^L \phi_{j-1}\cdot\phi_j\,dx = \int_{-\Delta x}^{\Delta x} \phi_L\cdot\phi_C\,dx$$

$$= \int_{-\Delta x}^{\Delta x} \left[-\tfrac{1}{2}\cdot\tfrac{x}{\Delta x} + \tfrac{1}{2}\cdot(\tfrac{x}{\Delta x})^2 \right]\cdot\left[1 - (\tfrac{x}{\Delta x})^2 \right] dx$$

$$= \int_{-1}^{1} \left(-\tfrac{1}{2}\cdot\xi + \tfrac{1}{2}\cdot\xi^2 \right)\cdot\left(1 - \xi^2 \right)\cdot\Delta x\,d\xi \qquad \left(\xi = \tfrac{x}{\Delta x} \right)$$

$$= \tfrac{2\Delta x}{15} .$$

Also,

$$\int_0^L \phi'_{j-1}\cdot\phi'_j\,dx = \int_{-\Delta x}^{\Delta x} \phi'_L\cdot\phi'_C\,dx$$

$$= \int_{-\Delta x}^{\Delta x} \left[-\tfrac{1}{2}\cdot\tfrac{1}{\Delta x} + \tfrac{x}{\Delta x^2} \right]\cdot\left[-\tfrac{2x}{\Delta x^2} \right] dx$$

$$= \int_{-1}^{1} \left(-\tfrac{1}{2} + \xi\right)\cdot\left(-2\xi \right)\,d\xi \qquad \left(\xi = \tfrac{x}{\Delta x} \right)$$

$$= -\tfrac{4}{3}\cdot\tfrac{1}{\Delta x} .$$

In a similar fashion, we can evaluate the other integrals.

Thus, for j odd, we have

$$0 = c^2 \cdot \left(-\frac{4}{3\Delta x}\, u_{j-1}(t) + \frac{8}{3\Delta x} \cdot u_j(t) - \frac{4}{3\Delta x}\, u_{j+1}(t)\right)$$

$$+ \left(\frac{2\Delta x}{15} \cdot u''_{j-1}(t) + \frac{16\Delta x}{15} \cdot u''_j(t) + \frac{2\Delta x}{15} \cdot u''_{j+1}(t)\right). \qquad (6.3)$$

Consider (6.2). Figure 6.2 is a graph of ϕ_{j-2}, ϕ_{j-1}, ϕ_j, ϕ_{j+1}, and ϕ_{j+2} over the support of ϕ_j for j even.

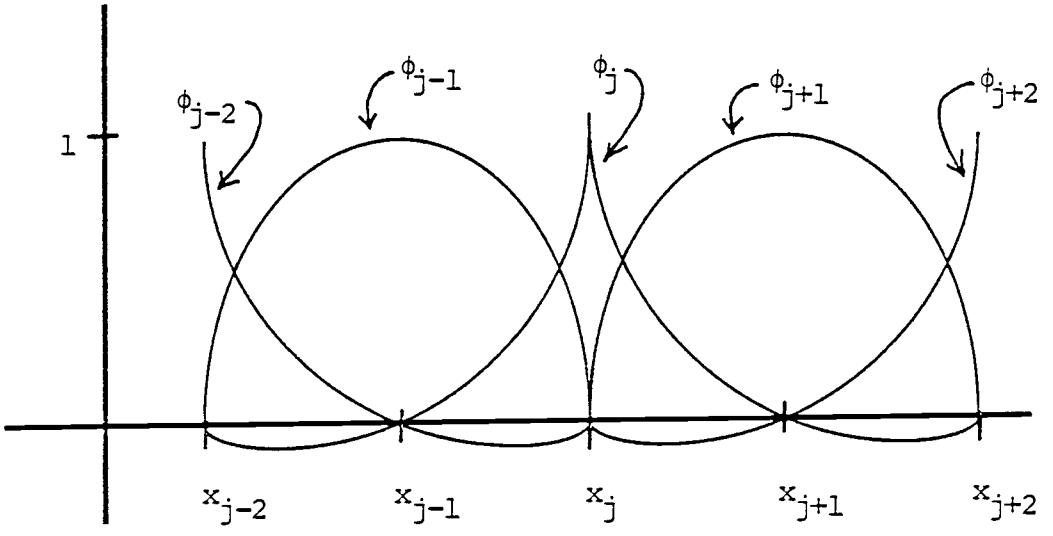

Figure 6.2. The graphs of ϕ_{j-2}, ϕ_{j-1}, ϕ_j, ϕ_{j+1}, and ϕ_{j+2}, j even. This is graphed over the support of ϕ_j.

To evaluate each integral, we do the same as we did for (6.1). For example, to evaluate

$$\int_0^L \phi_{j-2} \cdot \phi_j \, dx \,,$$

we shift the graphs of ϕ_{j-2} and ϕ_j (see Figure 6.3) to-

wards the origin.

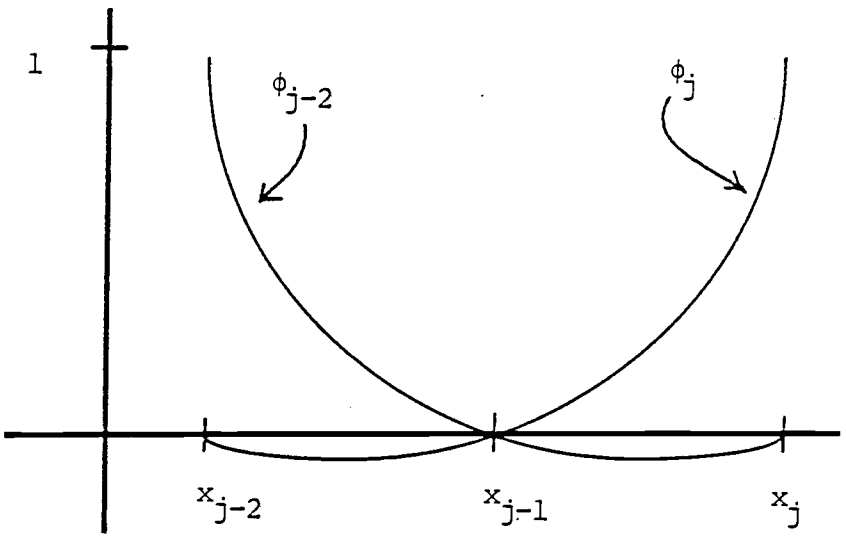

Figure 6.3. The graphs of ϕ_{j-2} and ϕ_j, j even.

Thus,

$$\int_0^L \phi_{j-2} \cdot \phi_j \, dx = \int_{-\Delta x}^{\Delta x} \phi_L \cdot \phi_R \, dx$$

$$= \int_{-\Delta x}^{\Delta x} \left[-\tfrac{1}{2}\cdot\tfrac{x}{\Delta x} + \tfrac{1}{2}\cdot\left(\tfrac{x}{\Delta x}\right)^2 \right] \cdot \left[\tfrac{1}{2}\cdot\tfrac{x}{\Delta x} + \tfrac{1}{2}\cdot\left(\tfrac{x}{\Delta x}\right)^2 \right] dx$$

$$= -\tfrac{\Delta x}{15}$$

where again, we use the substitution $\xi = \frac{x}{\Delta x}$.

To evaluate $\int_0^L \phi_j^2 \, dx$,we are looking at Figure 6.4.

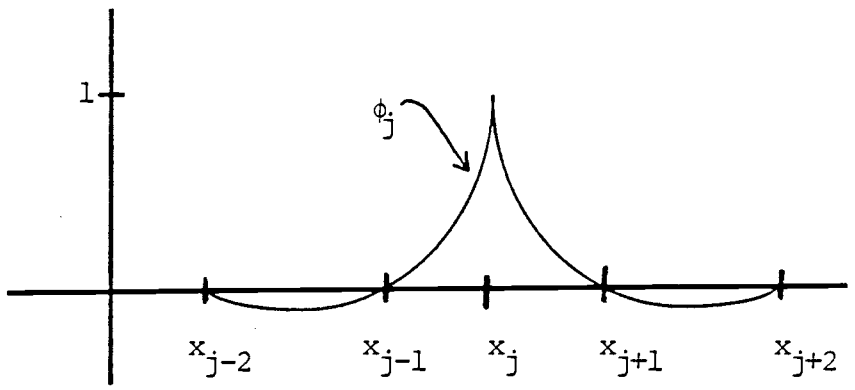

Figure 6.4. The graph of ϕ_j, j even.

So,

$$\int_0^L \phi_j^2 \, dx = 2 \cdot \int_{-\Delta x}^{\Delta x} \phi_R^2 \, dx$$

$$= \frac{8\Delta x}{15} .$$

Continuing in this manner, we get for j even

$$0 = c^2 \cdot \left(\frac{1}{6\Delta x} \cdot u_{j-2}(t) - \frac{4}{3\Delta x} \cdot u_{j-1}(t) + \frac{7}{3\Delta x} \cdot u_j(t) - \frac{4}{3\Delta x} \cdot u_{j+1}(t) + \frac{1}{6\Delta x} \cdot u_{j+2}(t) \right) + \left(-\frac{\Delta x}{15} \cdot u''_{j-2}(t) + \frac{2\Delta x}{15} \cdot u''_{j-1}(t) + \frac{8\Delta x}{15} \cdot u''_j(t) + \frac{2\Delta x}{15} \cdot u''_{j+1}(t) - \frac{\Delta x}{15} \cdot u''_{j+2}(t) \right). \quad (6.4)$$

To look for an integral form for $u_j(t)$ such that it will solve both (6.3) and (6.4) is too difficult to do. The best that we can do is to obtain a numerical computing scheme from (6.3) and (6.4) and use it on our test problem from section 4.

To obtain our computing scheme from (6.3) and (6.4),

we approximate $u_j''(t)$ in the usual way. Call these computing schemes (6.5) and (6.6), respectively. Since we will have implicit schemes, we end up with a matrix equation $A\hat{x} = \hat{b}$ where A is a five band matrix with altering lines

$$\left[0, \frac{2}{15}, \frac{16}{15}, \frac{2}{15}, 0\right] \text{ and } \left[\frac{1}{15}, -\frac{2}{15}, -\frac{8}{15}, -\frac{2}{15}, \frac{1}{15}\right],$$

$\hat{x}$ is the numerical approximations at time level n, and $\hat{b}$ is a vector obtained by using the approximations from time level (n-1).

Figure 6.5 is a graph of the results for our test problem with $\nu = 0.5$ and $t = 2$. Notice how much less dispersion has occurred compared to Figures 5.7 and 4.6. Thus, we see that the quadratic finite element method causes less dispersion to occur than the second order centered finite difference method and the linear finite element method.

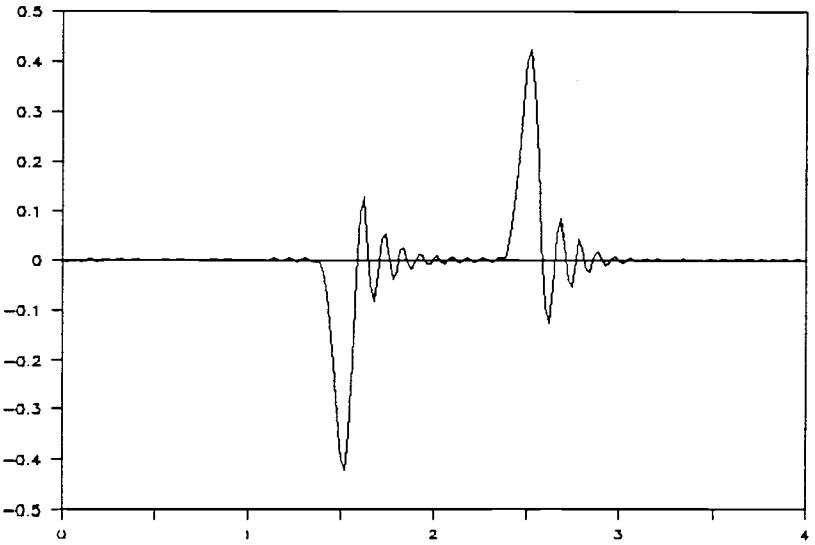

Figure 6.5. Test problem for u_j^n, $\nu=0.5$. The graph of (6.5) and (6.6) for the test problem with $\nu=0.5$, $n=199$.

7. THE REVISED LINEAR FINITE ELEMENT METHOD IN 1-D

We will now try an experiment that will give some unexpected results.

In section 6, we came up with two equations, (6.3) and (6.4), that made up the quadratic finite element approximation scheme. Consider (6.3). It is indexed in j where j is an odd integer. Define

$$0 = \left(\frac{c}{\Delta x}\right)^2 \cdot \left(u_{j+1}(t) - 2 \cdot u_j(t) + u_{j-1}(t) \right) - \left(\frac{1}{10} \cdot u''_{j-1}(t) + \frac{4}{5} \cdot u''_j(t) + \frac{1}{10} \cdot u''_{j+1}(t) \right) \quad (7.1)$$

for all values of j. This equation looks like the true linear finite element approximation scheme with different constants. Therefore, we will call (7.1) the revised linear finite element approximation scheme. Although (7.1) cannot be obtained in any usual finite element process, it can still be analyzed using the methods developed in the preceding sections.

After much work, we obtain E_{gv},

$$E_{gv} = \left| \frac{5 \cdot \sqrt{10}}{2} \cdot \frac{\sin|k|\Delta x}{(4+\cos k\Delta x)^{3/2}} \cdot \frac{1}{(1-\cos k\Delta x)^{1/2}} - 1 \right|. \quad (7.2)$$

Figure 7.1 is a graph of (7.2) for N=6,...,25. For $N \geq 10$, the graph of (7.2) will fall below the 1% level. A comparison of the graph of (7.2) with (5.5) and (4.8) shows that

(7.2) goes to zero at a much quicker rate as N→∞. Thus, the approximation method used to obtain (7.1) is superior to the methods of the previous sections.

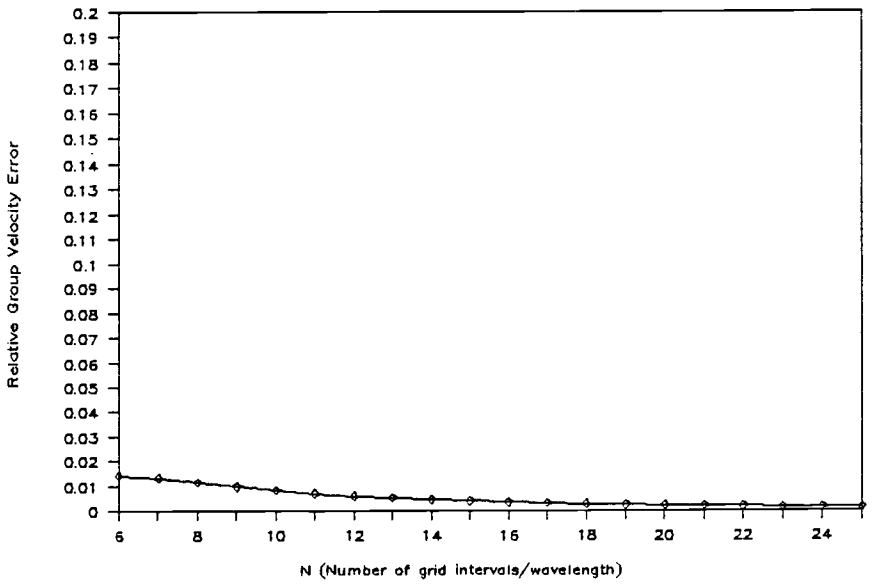

Figure 7.1. E_{gv} for $u_j(t)$, N=6,...,25. The graph of (7.2) as a function of N where N=6,...,25. The results from this graph indicate that (7.2) is a better approximation scheme than any of the previous methods.

Replace $u_j''(t)$ with the usual second order approximation and (7.1) becomes the numerical computing scheme

$$0 = \nu^2\cdot(u_{j+1}^n - 2\cdot u_j^n + u_{j-1}^n) - \frac{1}{10}\cdot(u_{j-1}^{n+1} - 2\cdot u_{j-1}^n + u_{j-1}^{n-1})$$

$$- \frac{4}{5}\cdot(u_j^{n+1} - 2\cdot u_j^n + u_j^{n-1}) - \frac{1}{10}\cdot(u_{j+1}^{n+1} - 2\cdot u_{j+1}^n + u_{j+1}^{n-1}). \qquad (7.3)$$

In order to analyze stability, we proceed as before. We eventually end with

$$(\cos k\Delta x + 4)z - 8 + (\cos k\Delta x + 4)z^{-1} = -20\cdot\nu^2\cdot\sin^2\tfrac{k\Delta x}{2} + 2\cdot\cos k\Delta x. \qquad (7.4)$$

Set

$$f(z) = (\cos k\Delta x + 4)z - 8 + (\cos k\Delta x + 4)z^{-1} .$$

The range of f for z real is

$$(-\infty\ ,\ -2(4+\cos k\Delta x) - 8\ ] \ \cup\ [\ 2(4+\cos k\Delta x) - 8\ ,\ \infty\ ).$$

As before, we want to bound ν such that

$$\begin{aligned} -2(4+\cos k\Delta x) - 8 \quad &\le \quad -20\cdot\nu^2\cdot\sin^2\tfrac{k\Delta x}{2} + 2\cdot\cos k\Delta x \\ &\le \quad 2(4+\cos k\Delta x) - 8. \end{aligned} \qquad (7.5)$$

The first inequality of (7.5) yields

$$\nu^2 \quad \le \quad \frac{16 + 4\cdot\cos k\Delta x}{20\cdot\sin^2\frac{k\Delta x}{2}} .$$

This holds true for all $k\Delta x$ if we require that $\nu \le \sqrt{\frac{3}{5}}$. Next, consider the second inequality of (7.5). It yields $\nu \ge 0$, which will always be true by definition of ν. Therefore, we require $\nu \le \sqrt{\frac{3}{5}}$.

Eventually, we end up with the group velocity error equation

$$E_{gv} = \qquad (7.6)$$

$$\left| \frac{10}{\sqrt{20(\cos k\Delta x+4) - 100\cdot\nu^2\cdot\sin^2\frac{k\Delta x}{2}}} \cdot \frac{\cos\frac{k\Delta x}{2}(\cos k\Delta x+4) + \sin\frac{|k|\Delta x}{2}\cdot\sin|k|\Delta x}{\cos k\Delta x + 4} - 1 \right| .$$

We now require $\nu < \sqrt{\frac{3}{5}}$ to avoid division by zero. For $\nu = 0.5$, the graph of (7.6) drops below 1% if $N \ge 15$. See Figure 7.2 where we graph (7.6) for $N = 6, \ldots, 25$. Thus, we expect this new numerical approximation scheme to give much better results than any of the previous schemes.

Figure 7.3 is a graph of the results for our test problem using the scheme with ν=0.5 and t=2. Notice how much less unwanted oscillations occurs in this graph when we compare it to Figures 6.5, 5.7, and 4.6.

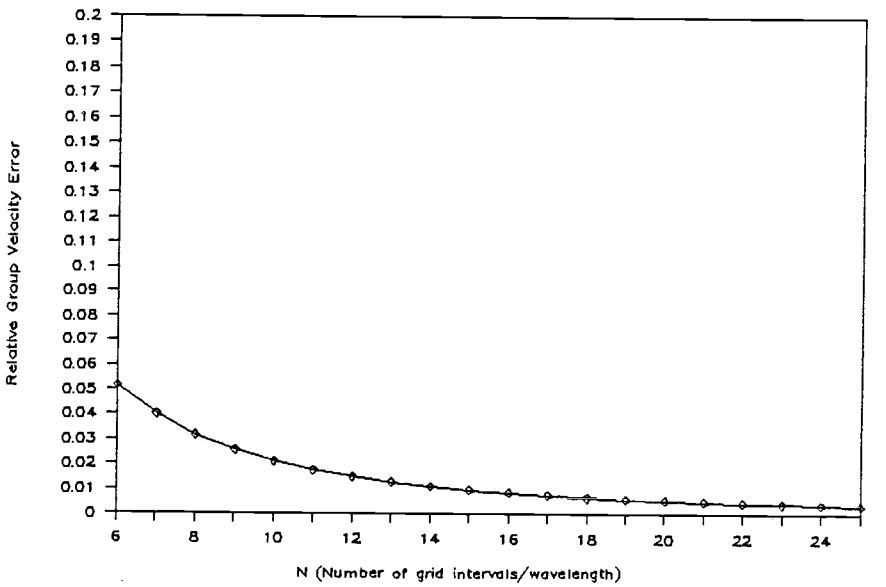

Figure 7.2. E_{gv} for u_j^n, ν=0.5, N=6,...,25. The graph of (7.6) as a function of N where N=6,...,25, ν=0.5. The curve is below the 1% level for N≥15. This fact tells us that (7.6) will be a better numerical computing scheme than the previous schemes.

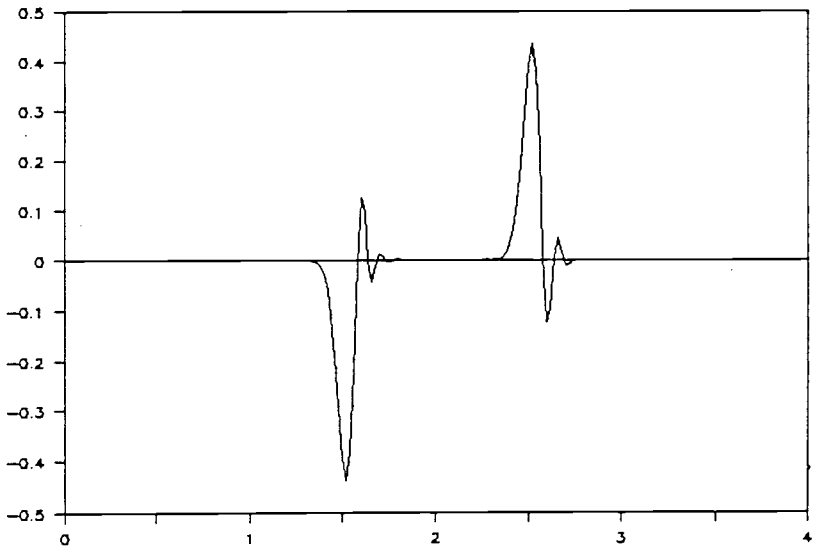

Figure 7.3. Test problem for u_j^n, ν=0.5. The graph of (7.3) for the test problem where ν=0.5 and n=199. The amount of dispersion is significantly less if we compare this figure to those from previous sections.

8. THE FOURTH ORDER CENTERED FINITE DIFFERENCE METHOD IN 1-D

We will develop a fourth order approximation to the spatial derivatives in the wave equation.

Let x_j be a point in the domain of a function f and suppose that $f^{(6)}$ exists in a neighborhood of x_j.

Defining $D^+f(x_j)$ and $D^-f(x_j)$ as we did in section 4, we get

$$D^+D^-(\Delta x)\ f(x_j) = \frac{1}{\Delta x^2}\cdot[\ f(x_j+\Delta x) - 2\cdot f(x_j) + f(x_j-\Delta x)\ ]$$

where the symbol (Δx) has been inserted to explicitly show the step size used. Also from section 4, we showed that

$$D^+D^-(\Delta x)\ f(x_j) = f''(x_j) + \frac{\Delta x^2}{12}\cdot f^{(4)}(x_j) + O(\Delta x^4) \quad (8.1)$$

Similarly, if we use the step size $2\Delta x$, we obtain

$$D^+D^-(2\Delta x)\ f(x_j) = f''(x_j) + \frac{\Delta x^2}{3}\cdot f^{(4)}(x_j) + O(\Delta x^4) \quad (8.2)$$

Since f(x) was arbitrary, we replace it with u(x,t), the solution to the wave equation for t fixed. Multiply (8.1) by 4 and subtract (8.2) from it. We get

$$u_{xx}(x_j,t) = \frac{4}{3}\cdot\left[\frac{u(x_j+\Delta x,t) - 2\cdot u(x_j,t) + u(x_j-\Delta x,t)}{\Delta x^2}\right]$$

$$- \frac{1}{3}\cdot\left[\frac{u(x_j+2\Delta x,t) - 2\cdot u(x_j,t) + u(x_j-2\Delta x,t)}{(2\Delta x)^2}\right] + O(\Delta x^4).$$

Let $u_j(t)$ approximate $u(x_j,t)$ and we obtain the fourth order centered finite difference approximation scheme

$$u_j''(t) =$$

$$c^2\cdot\left[\frac{4}{3}\cdot\left[\frac{u_{j+1}(t)-2\cdot u_j(t)+u_{j-1}(t)}{\Delta x^2}\right]-\frac{1}{3}\cdot\left[\frac{u_{j+2}(t)-2\cdot u_j(t)+u_{j-2}(t)}{(2\Delta x)^2}\right]\right] \qquad (8.3)$$

with group velocity error equation

$$E_{gv} = \left|\frac{1}{\sqrt{6}}\cdot\frac{8\cdot\sin|k|\Delta x-\sin 2|k|\Delta x}{\sqrt{16\cdot\sin^2\frac{k\Delta x}{2}-\sin^2 k\Delta x}}-1\right|. \qquad (8.4)$$

Consider the graph of (8.4) in Figure 8.1. A comparison of Figure 8.1 with Figures 7.1, 5.4, and 4.2 shows that (8.4) and (7.2) go to zero (as $N\to\infty$) at about equal rates while (5.5) and (4.8) go to zero at a slower rate.

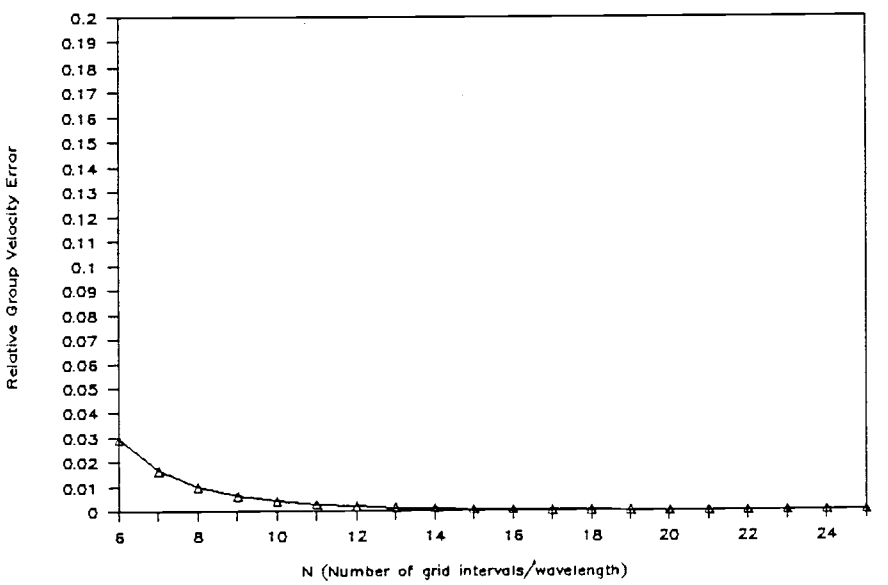

Figure 8.1. E_{gv} for $u_j(t)$, $N=6,\ldots,25$. The graph of (8.4) as a function of N where $N=6,\ldots,25$.

From (8.3), we get the numerical computing scheme

$$0 = \nu^2\cdot\left[\frac{4}{3}\cdot(u_{j+1}^n - 2\cdot u_j^n + u_{j-1}^n) - \frac{1}{12}\cdot(u_{j+2}^n - 2\cdot u_j^n + u_{j-2}^n)\right]$$

$$- (u_j^{n+1} - 2\cdot u_j^n + u_j^{n-1}). \qquad (8.5)$$

From our stability analysis, we find

$$z - 2 + z^{-1} = \frac{\nu^2}{3}\cdot(\sin^2\frac{k\Delta x}{2} - 16\cdot\sin^2 k\Delta x).$$

We need a bound on ν to ensure that there are no roots outside the unit circle. Proceeding as before, we set

$$f(z) = z - 2 + z^{-1}.$$

Since the range of f is $(-\infty,-4]\cup[0,\infty)$, we want to bound ν such that

$$-4 \le -\frac{\nu^2}{3}\cdot\left[16\cdot\sin^2\frac{k\Delta x}{2} - \sin^2 k\Delta x\right] \le 0$$

or $\nu \le \frac{\sqrt{3}}{2}$. For the group velocity error equation, obtain

$$E_{gv} = \left|\frac{8\cdot\sin|k|\Delta x - \sin 2|k|\Delta x}{\sqrt{12\cdot(16\cdot\sin^2\frac{k\Delta x}{2} - \sin^2 k\Delta x) - \nu^2\cdot(16\cdot\sin^2\frac{k\Delta x}{2} - \sin^2 k\Delta x)^2}} - 1\right| \qquad (8.6)$$

where now we have $\nu<\frac{\sqrt{3}}{2}$.

For more information on fourth order methods, see [Shubin and Bell].

When $\nu=0.5$, we need $N\ge4$ for (8.6) to fall below the

1% level. Figure 8.2 is the graph of (8.6) for N=6,...,25. Thus, we expect (8.5) to be the most accurate of all the schemes we have studied.

Figure 8.3 is a graph of the numerical approximations from (8.5) for the same test problem as before with $\nu=0.5$ and t=2. The amount of dispersion found in Figure 8.3 is quite small compared to the previous figures.

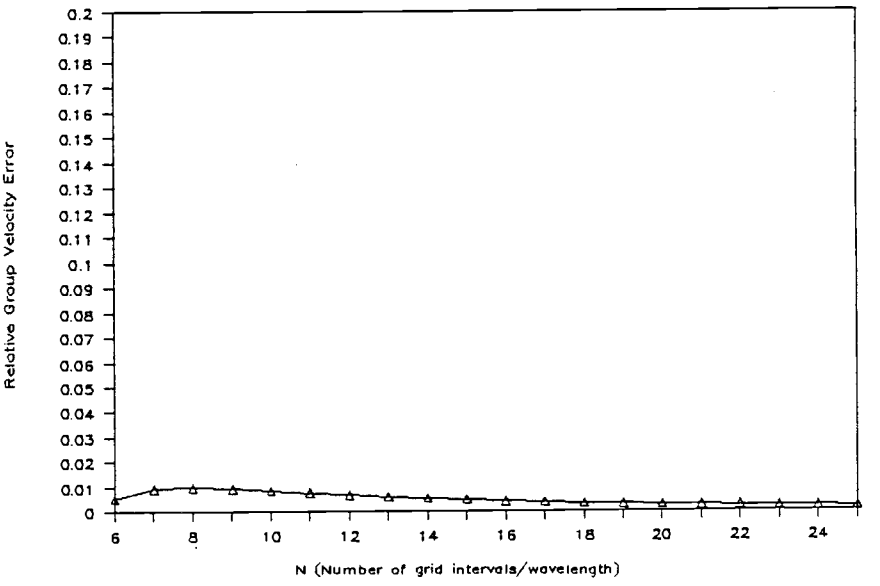

Figure 8.2. E_{gv} for u_j^n, $\nu=0.5$, N=6,...,25. The graph of (8.6) as a function of N where N=6,...,25, $\nu=0.5$. We cannot determine from this figure but (8.6) is less than 0.01 for $N\geq 4$.

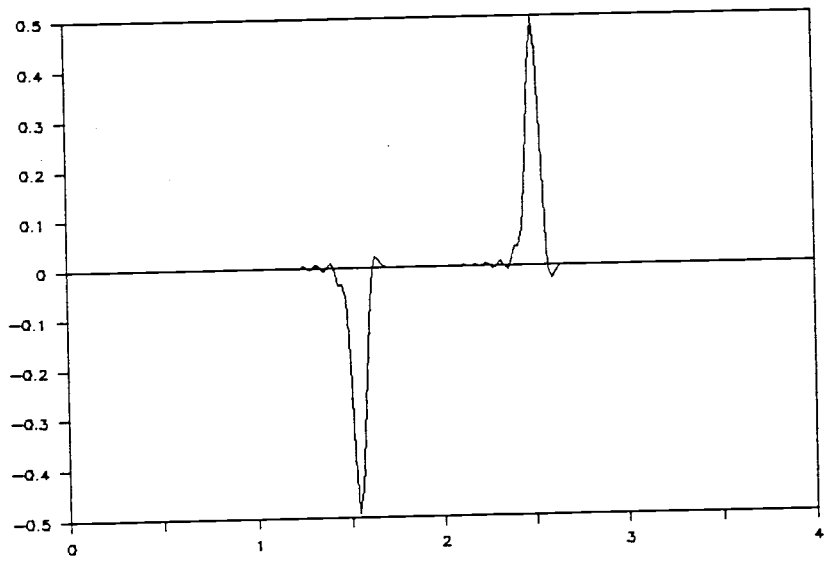

Figure 8.3. Test problem for u_j^n, $\nu=0.5$. The graph of (8.5) for the test problem where $\nu=0.5$, $n=199$. Clearly, the amount of dispersion occurring here is much less compared to previous results.

9. SUMMARY FOR THE 1-D CASE

Consider the graphs of the relative group velocity error equations for the time continuous approximation schemes. Both the second order centered finite difference method and the linear finite difference method are equally effective because the graphs for equations (4.8) and (5.5) are very similar to each other. Equations (7.2) and (8.4) both have graphs quite similar to each other and so we can conclude that the revised linear finite element method and the fourth order centered finite difference method approximate the spatial derivative in the wave equation with about the same degree of accuracy.

The fourth order centered finite difference method has an error of order four and so even beginning our work, we would expect it to be a superior method to the second order centered finite difference method. The surprise of this analysis is how much better the revised linear finite element method did over the the true linear finite element method.

Next, consider the numerical computing schemes. Choosing the best scheme of the four is not difficult. For ease in programming and accuracy in the numerical approximations, equation (8.5) is the best. Not only is it fourth order accurate in space but is also an explicit scheme. Al-

though equation (7.3) is of similar accuracy, it is not an explicit scheme and so is harder to program. Equation (4.9) would be a better choice over (5.6) (even if they both have similar accuracy levels) because (4.9) is an explicit scheme.

10. GROUP AND PHASE VELOCITY IN TWO DIMENSIONS

Consider a two-dimensional propagating wave of the form

$$u(x,y,t) = \int_c^d \int_a^b f(\xi,\eta)\cdot e^{i(\xi x+\eta y-\omega t)}\, d\xi\, d\eta \qquad (10.1)$$

where f is a bounded, real-valued amplitude function and $\omega=\omega(\xi,\eta)$. Call the function relating ω with ξ and η the dispersion relation for u.

We will define the group and phase velocity vectors for u. Let ξ_0 be a point between a and b, η_0 a point between c and d. We will assume $|\xi_0| \gg (b-a)$ and $|\eta_0| \gg (d-c)$. Define $\omega_0=\omega(\xi_0,\eta_0)$ and consider

$$u(x,y,t) = e^{i(\xi_0 x+\eta_0 y-\omega_0 t)}\cdot \int_c^d \int_a^b f(\xi,\eta)\cdot e^{i[(\xi-\xi_0)x+(\eta-\eta_0)y-(\omega-\omega_0)t]}\, d\xi\, d\eta.$$

Using Taylor's theorem in 2-D, we have

$$\omega(\xi,\eta)-\omega(\xi_0,\eta_0) =$$

$$(\xi-\xi_0)\,\frac{\partial}{\partial\xi}\omega(\xi_0,\eta_0) + (\eta-\eta_0)\,\frac{\partial}{\partial\eta}\omega(\xi_0,\eta_0) + O\left[\,|\xi-\xi_0| + |\eta-\eta_0|\,\right]^2.$$

So,

$$u(x,y,t) \approx e^{i(\xi_0 x+\eta_0 y-\omega_0 t)}\cdot F[x-\omega_\xi(\xi_0,\eta_0)t,\, y-\omega_\eta(\xi_0,\eta_0)t] \qquad (10.2)$$

where

$$F = \int_c^d \int_a^b f(\xi,\eta)\cdot e^{i(\xi-\xi_0)[x-\omega_\xi(\xi_0,\eta_0)t] + i(\eta-\eta_0)[y-\omega_\eta(\xi_0,\eta_0)t]}\, d\xi\, d\eta.$$

We define the group and phase velocity vectors for (10.2). The observations on (10.2) are similar to those found in section 2 and in most cases, their justifications will be omitted. To define the group and phase velocity vectors for (10.2), we will need the velocity vectors for its complex exponential part and for F. For F, the velocity vector is $(\omega_\xi(\xi_0,\eta_0),\omega_\eta(\xi_0,\eta_0))$. To determine the velocity vector for the complex exponential part of (10.2), we will determine the velocity vector for its real and imaginary parts. The complex exponent of (10.2) has real part

$$\cos(\xi_0 x+\eta_0 y-\omega_0 t) = \cos|(\xi_0,\eta_0)|\,[\mathcal{R}\cdot(x,y)-\mathcal{C}t] \quad (10.3)$$

where

$$\mathcal{R} = \frac{(\xi_0,\eta_0)}{|(\xi_0,\eta_0)|}, \quad \mathcal{C} = \frac{\omega_0}{|(\xi_0,\eta_0)|}.$$

Consider an arbitrary point (x,y). We look at $\mathcal{R}$ and $\mathcal{R}\cdot(x,y)$ on the xy-plane. See Figure 10.1. For every point (x,y), there is a point on L that is $\mathcal{R}\cdot(x,y)$ distance away from the origin. The graph of (10.3) as a function of $\mathcal{R}\cdot(x,y)$ is a cosine wave (t fixed). See Figure 10.2.

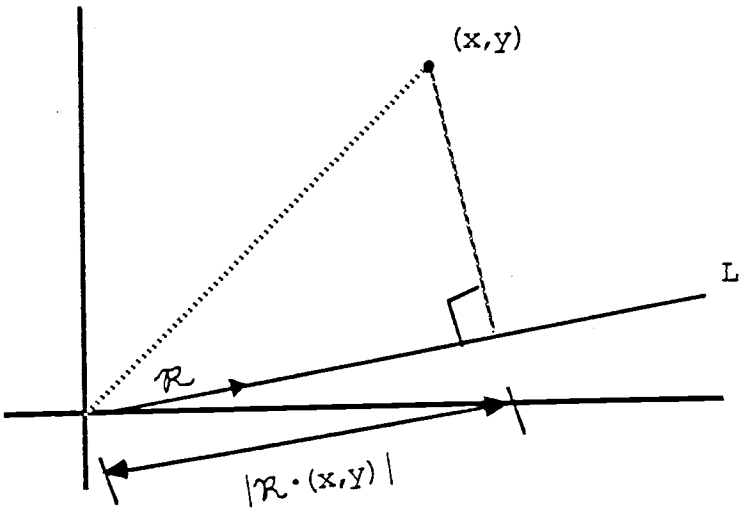

Figure 10.1. The arbitrary point (x,y) with $\mathcal{R}\cdot(x,y)$ and $|\mathcal{R}\cdot(x,y)|$.

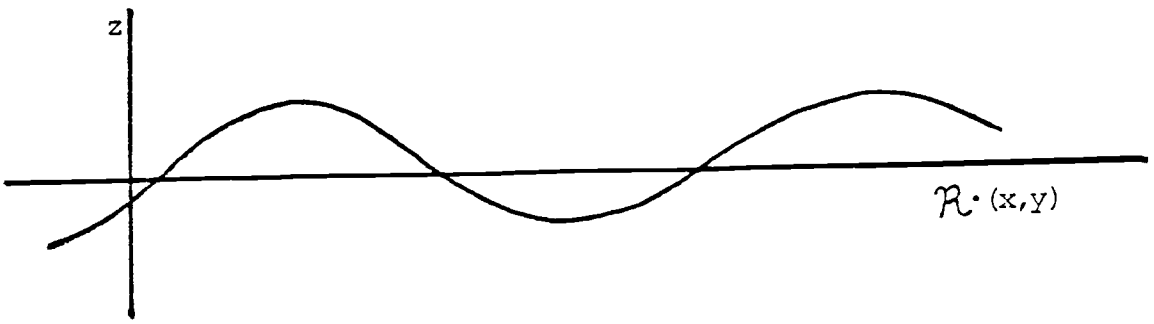

Figure 10.2. The graph of $\cos|(\xi_0,\eta_0)|\,[\mathcal{R}\cdot(x,y)-Ct]$ as a function of $\mathcal{R}\cdot(x,y)$.

Thus, (10.3) as function of x and y with t fixed looks like a cosine wave in 3-D. See Figure 10.3.

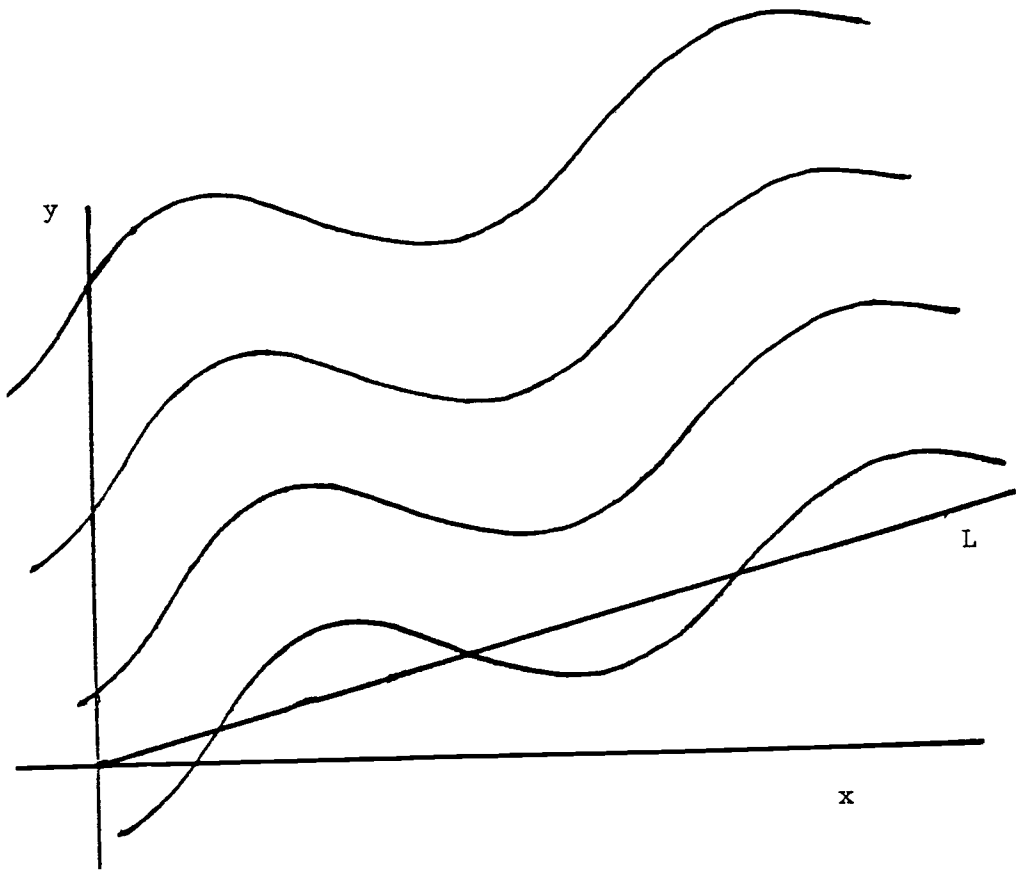

Figure 10.3. The graph of $\cos|(\xi_0,\eta_0)|\,[\mathcal{R}\cdot(x,y)-\mathcal{C}t]$ as a function of x and y. The graph is a three dimensional figure cutting back and forth through the xy-plane.

Thus, the graph for t fixed of

$$\cos|(\xi_0,\eta_0)|\,[\mathcal{R}\cdot(x,y)-\mathcal{C}t]$$

is just the graph of

$$\cos|(\xi_0,\eta_0)|\,[\mathcal{R}\cdot(x,y)]$$

translated $\mathcal{C}t$ units along the line L.

We summarize. Equation (10.3) has a graph that moves in the direction $\frac{(\xi_0,\eta_0)}{|(\xi_0,\eta_0)|}$ with speed $|\mathcal{C}|$. Therefore, it has a velocity vector

$$\mathcal{C}\cdot\frac{(\xi_0,\eta_0)}{|(\xi_0,\eta_0)|} = \frac{\omega_0}{|(\xi_0,\eta_0)|^2}(\xi_0,\eta_0). \tag{10.4}$$

The complex exponent of (10.2) has imaginary part $\sin(\xi_0x+\eta_0y-\omega_0t)$. It will have a velocity vector of the form (10.4). We conclude that the complex exponential part of (10.2) has a velocity vector (10.4).

Next, consider the graphs of F and the complex exponential term in (10.2) for t fixed. It can be shown that the graph of F is a slow varying one compared to the graph of the complex exponential. Thus, the graph of u is made up of a complex exponential wave embedded in an envelope of the form of F. The group velocity vector for u, $\overline{C}_g$, will be defined to be the velocity vector of the envelope. Thus,

$$\overline{C}_g = (\omega_\xi(\xi_0,\eta_0)\ ,\ \omega_\eta(\xi_0,\eta_0))\ . \tag{10.5}$$

The phase velocity vector, $\overline{C}_p$, for u will be defined to be the velocity vector for the wave in the envelope. Thus,

$$\overline{C}_p = \frac{\omega_0}{|(\xi_0, \eta_0)|^2}(\xi_0, \eta_0) \cdot$$

Consider a more general form for (10.1) where (b−a) and (d−c) are both of arbitrary size. We deal with u as follows. Divide [a,b] and [c,d] into tiny intervals by

$$a = \alpha_0 < \alpha_1 < \alpha_2 < \cdots < \alpha_{M-1} < \alpha_M = b$$

and

$$c = \beta_0 < \beta_1 < \cdots < \beta_N = d$$

where M and N are both arbitrary integers. We can thus write (10.1) as

$$u(x,y,t) = \sum_{r=1}^{N} \sum_{q=1}^{M} \int_{\beta_{r-1}}^{\beta_r} \int_{\alpha_{q-1}}^{\alpha_q} f(\xi, \eta) \cdot e^{i(\xi x + \eta y - \omega t)} \, d\xi \, d\eta .$$

Each integral represents a travelling wave with the (qth, rth) integral having a group velocity vector of the form (10.5) where $\alpha_{q-1} \leq \xi_0 \leq \alpha_q$ and $\beta_{r-1} \leq \eta_0 \leq \beta_r$. We think of u as a superposition of many waves, each wave having a particular group velocity vector. These waves may travel at various speeds and directions.

11. SOLUTIONS TO THE TWO-DIMENSIONAL WAVE EQUATION

Consider the two-dimensional wave equation

$$u_{tt} = c^2 \cdot (u_{xx} + u_{yy})$$

for given initial conditions. Its solution can be represented in an integral form using the dispersion relation

$$\omega^2 = c^2 \cdot (\xi^2 + \eta^2) .$$

Since the vector

$$\left[\pm \frac{c\xi}{\sqrt{\xi^2+\eta^2}} \ , \ \pm \frac{c\eta}{\sqrt{\xi^2+\eta^2}} \right]$$

is both the group and phase velocity vector, the solution to the wave equation will not disperse. The angle

$$\phi = \tan^{-1} \left| \frac{\omega_\eta}{\omega_\xi} \right| = \tan^{-1} \left| \frac{\eta}{\xi} \right| \ ,$$

is the smaller angle made between the group velocity vector for the wave with wave number vector (ξ, η) and the x-axis. We will call this the group propagation angle. It gives us an idea of what directions the waves with wave number vectors $(\pm\xi, \pm\eta)$ are travelling. Like before, we will compare the group velocity vectors for different numerical schemes with the group velocity vector for a general solution to the wave equation.

12. THE SECOND ORDER CENTERED FINITE DIFFERENCE METHOD IN 2-D

We now begin analyzing various approximation methods applied to the 2-D wave equation starting with the second order centered finite difference method in 2-D. Let $u(x,y,t)$ be the solution to the wave equation for given initial conditions. As in the one dimensional sections, we will consider only the IVP for the wave equation in order to eliminate the need to incorporate boundary effects. Let $u_{j,m}(t)$ approximate $u(j\Delta x, m\Delta y, t)$. Since

$$u_{xx}(x,y,t) = \frac{1}{\Delta x^2}\cdot\left[\, u(x+\Delta x,y,t) - 2\cdot u(x,y,t) + u(x-\Delta x,y,t)\,\right] + O(\Delta x^2)$$

and

$$u_{yy}(x,y,t) = \frac{1}{\Delta y^2}\cdot\left[\, u(x,y+\Delta y,t) - 2\cdot u(x,y,t) + u(x,y-\Delta y,t)\,\right] + O(\Delta y^2),$$

we have the second order centered finite difference approximation scheme

$$0 = c^2\cdot\left[\frac{u_{j+1,m}(t) - 2\cdot u_{j,m}(t) + u_{j-1,m}(t)}{\Delta x^2} + \frac{u_{j,m+1}(t) - 2\cdot u_{j,m}(t) + u_{j,m-1}(t)}{\Delta y^2}\right]$$

$$- \frac{d^2}{dt^2}u_{j,m}(t). \qquad (12.1)$$

We need a form for $u_{j,m}(t)$. Define a Fourier transform of a grid function by

$$\hat{u}(\xi\Delta x, \eta\Delta y, t) = \Delta x\cdot\Delta y\cdot\sum_{m=-\infty}^{\infty}\sum_{j=-\infty}^{\infty} u_{j,m}(t)\cdot e^{-i(\xi\Delta x\cdot j + \eta\Delta y\cdot m)}$$

$$= \sum_{m=-\infty}^{\infty}\sum_{j=-\infty}^{\infty}(\Delta x\cdot\Delta y\cdot u_{j,m}(t))\cdot e^{-i(\xi\Delta x\cdot j + \eta\Delta y\cdot m)}.$$

Think of this as a Fourier series expansion for $\hat{u}$ in $\xi\Delta x$ and $\eta\Delta y$. Since $\hat{u}$ has a period of 2π in both $\xi\Delta x$ and $\eta\Delta y$, we restrict $-\pi \le \xi\Delta x \le \pi$ and $-\pi \le \eta\Delta y \le \pi$. If we regard $(\Delta x \cdot \Delta y \cdot u_{j,m}(t))$ as the coefficients in the series, then

$$u_{j,m}(t) = \frac{1}{4\pi^2} \int_{-\pi/\Delta y}^{\pi/\Delta y} \int_{-\pi/\Delta x}^{\pi/\Delta x} \hat{u}(\xi\Delta x, \eta\Delta y, t) \cdot e^{i(\xi\Delta x \cdot j + \eta\Delta y \cdot m)} \, d\xi \, d\eta. \qquad (12.2)$$

We need a form for $\hat{u}$. To get it, put (12.2) into (12.1) and using ideas from section 4, we obtain

$$0 = \left[\left(\frac{c}{\Delta x}\right)^2 \cdot (e^{i\xi\Delta x} - 2 + e^{-i\xi\Delta x}) + \left(\frac{c}{\Delta y}\right)^2 \cdot (e^{i\eta\Delta y} - 2 + e^{-i\eta\Delta y}) \right] \hat{u} - \hat{u}_{tt}.$$

Solving for $\hat{u}$, we get

$$\hat{u} = A(\xi, \eta) \cdot e^{-i\omega t} + B(\xi, \eta) \cdot e^{i\omega t}$$

where

$$\omega = \omega(\xi, \eta) = 2c \sqrt{\left(\frac{1}{\Delta x}\right)^2 \cdot \sin^2 \frac{\xi\Delta x}{2} + \left(\frac{1}{\Delta y}\right)^2 \cdot \sin^2 \frac{\eta\Delta y}{2}} \, .$$

Define $\omega_1 = \omega$ and $\omega_2 = -\omega$. Then,

$$u_{j,m}(t) = \frac{1}{4\pi^2} \cdot \int_{-\pi/\Delta y}^{\pi/\Delta y} \int_{-\pi/\Delta x}^{\pi/\Delta x} A(\xi, \eta) \cdot e^{i(\xi x + \eta y - \omega_1 t)} \, d\xi \, d\eta$$

$$+ \frac{1}{4\pi^2} \cdot \int_{-\pi/\Delta y}^{\pi/\Delta y} \int_{-\pi/\Delta x}^{\pi/\Delta x} B(\xi, \eta) \cdot e^{i(\xi x + \eta y - \omega_2 t)} \, d\xi \, d\eta \, .$$

To determine an accuracy level for the scheme (12.1),

we will consider $u_{j,m}(t)$ as a superposition of travelling waves. For each wave with wave number vector (ξ,η), we will determine its group speed $|\overline{C}_g|$, and its group propagation angle Θ, i.e., the smaller angle made between its group velocity vector and the x-axis. Thus, for

$$-\pi \le \xi\Delta x \le \pi \text{ and } -\pi \le \eta\Delta y \le \pi,$$

$$\Theta = \tan^{-1}\left|\frac{\Delta x}{\Delta y}\cdot\frac{\sin\eta\Delta y}{\sin\xi\Delta x}\right| , \tag{12.3}$$

$$|\overline{C}_g| = \frac{c}{\Delta x\cdot\Delta y}\cdot\frac{1}{2}\cdot\sqrt{\frac{\Delta y^2\cdot\sin^2\xi\Delta x + \Delta x^2\cdot\sin^2\eta\Delta y}{(\frac{1}{\Delta x})^2\cdot\sin^2\frac{\xi\Delta x}{2} + (\frac{1}{\Delta y})^2\cdot\sin^2\frac{\eta\Delta y}{2}}},$$

where $\Theta = \tan^{-1}\left|\frac{\omega_\eta}{\omega_\xi}\right|$ and $|\overline{C}_g| = \sqrt{\omega_\xi^2 + \omega_\eta^2}$. To simplify things, set $\Delta x = \Delta y = h$. So,

$$\Theta = \tan^{-1}\left|\frac{\sin\eta h}{\sin\xi h}\right|$$

$$|\overline{C}_g| = \frac{c}{2}\cdot\sqrt{\frac{\sin^2\xi h + \sin^2\eta h}{\sin^2\frac{\xi h}{2} + \sin^2\frac{\eta h}{2}}} .$$

Recall section 11 where we discussed the solution $u(x,y,t)$ to the wave equation. If we considered u in an integral form, then u is a superposition of waves each with a wave number vector (ξ,η). Each superposed wave will have a group speed $|c|$ and group propagation angle $\phi = \tan^{-1}\left|\frac{\eta}{\xi}\right|$. We will use these facts to quantitatively

look at Θ and $|\overline{C}_g|$.

First, we will consider Θ. Define N as follows. For a wave travelling in either the x or y direction, let

$$N = \frac{\lambda}{h} = \frac{2\pi/|k|}{h} = \frac{2\pi}{|k|h}$$

where λ is the wavelength of the wave and k is its wave number in the x or y direction. Therefore, N has the units of number of grid intervals per wavelength for waves moving in the x or y direction. Let N be an integer greater than 1. Consider the ξh-ηh plane with a circle of radius $\frac{2\pi}{N}$. Let ϕ be an angle between 0° and 90°. See Figure 12.1.

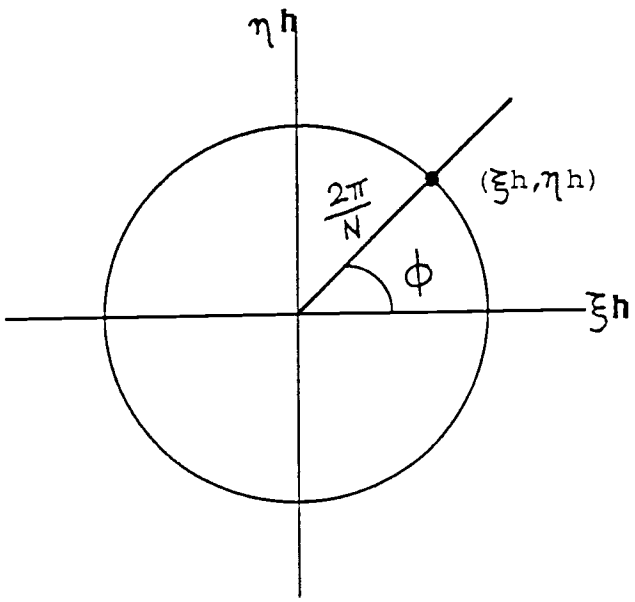

Figure 12.1. A circle of radius $\frac{2\pi}{N}$ in the ξh-ηh plane. We have N fixed and ϕ between 0° and 90°.

We have that

$$\xi h = \frac{2\pi}{N} \cdot \cos\phi$$

$$\eta h = \frac{2\pi}{N} \cdot \sin\phi .$$

The superposed wave of the true solution u with wave number vector (ξ,η) will travel with a group propagation angle of ϕ. The superposed wave of $u_{j,m}(t)$ with wave number vector (ξ,η) will have a group propagation angle of Θ. Thus, $|\phi-\Theta|$ is the group propagation angle error, i.e., the amount of degrees off from the correct angle the superposed wave of $u_{j,m}(t)$ should have travelled. We will let $N=2,3,\ldots$ and for each N, look at $|\phi-\Theta|$ for $\phi=0^\circ,\frac{1}{2}^\circ,1^\circ,\frac{3}{2}^\circ,\ldots,90^\circ$. Figure 12.2 is a graph for a few values of N. For each value of N, the superposed waves of $u_{j,m}(t)$ travel in the correct directions at 0°, 45°, and 90° and has its worst error at $22\frac{1}{2}^\circ$ and $67\frac{1}{2}^\circ$. Notice that as N gets bigger, the errors gets smaller. This means that as we let $\xi \to 0$ and $\eta \to 0$, waves with wave number vectors (ξ,η) travel with less and less error. Consider the graph corresponding to N=12 in Figure 12.2. We have that $|\phi-\Theta|$ is at most 0.67°. (We will always choose N=12 as a representative case in the comparison of different methods).

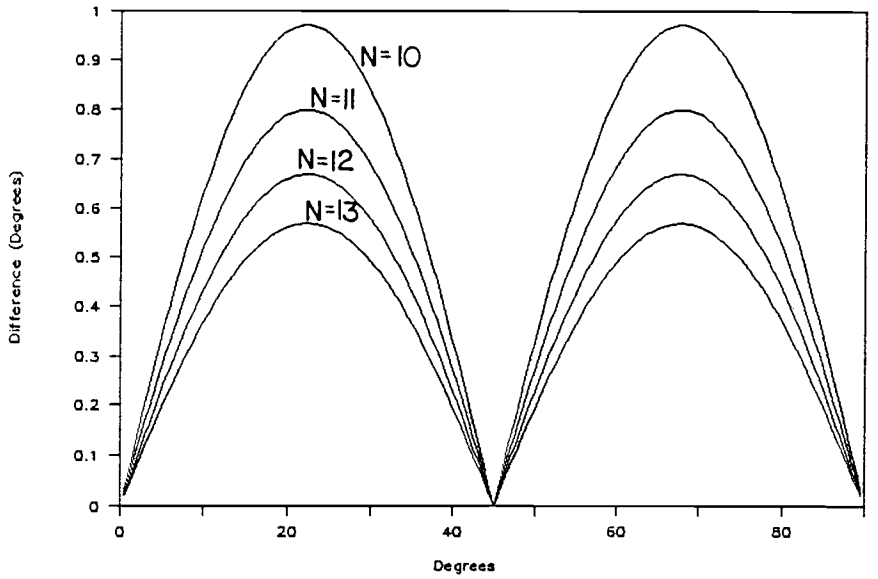

Figure 12.2. $|\phi-\Theta|$ for $u_{j,m}(t)$, N=10,...,13. The graph of $|\phi-\Theta|$ for (12.1) for N=10,...,13; ϕ is represented on the horizontal line. Each curve represents the group propagation angle error for waves with wave number vector (ξ,η), $\xi h = \frac{2\pi}{N}\cdot\cos\phi$, $\eta h = \frac{2\pi}{N}\cdot\sin\phi$.

Next, we look at $|\overline{C}_g|$. Once again, let ϕ be between 0° and 90° with ξh and ηh determined as above. The superposed wave of $u_{j,m}(t)$ with wave number vector (ξ,η) will travel with a speed of $|\overline{C}_g|$. Therefore, its relative group speed error E_s is

$$E_s = \left| \frac{|\overline{C}_g| - |c|}{|c|} \right| = \left| \frac{1}{2}\cdot\sqrt{\frac{\sin^2\xi h + \sin^2\eta h}{\sin^2\frac{\xi h}{2} + \sin^2\frac{\eta h}{2}}} - 1 \right| .$$

Figure 12.3 are graphs of E_s as a function of ϕ for different values of N. As N increases, i.e., as $\xi \to 0$ and $\eta \to 0$, the waves travel with less and less error in their group speed. For N=12, the curve lies within a 1.7 to 3.4% error span.

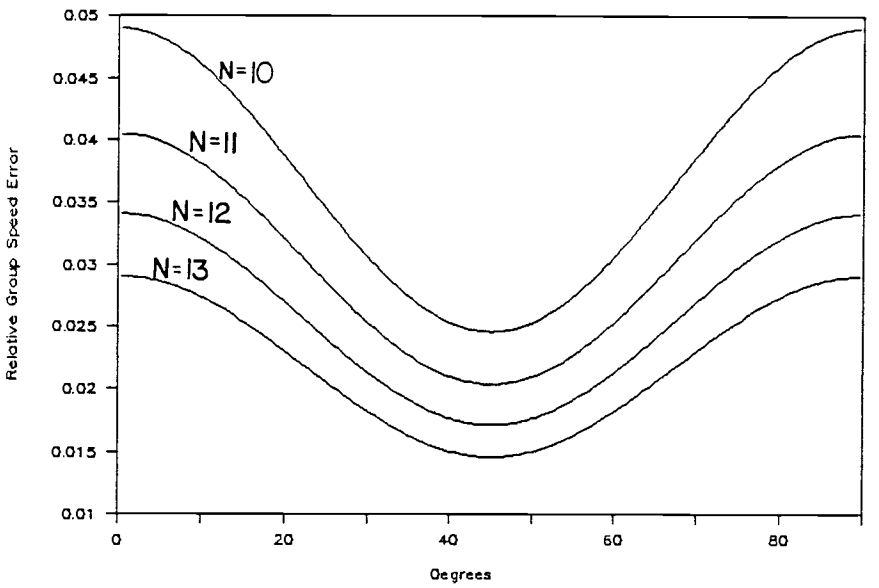

Figure 12.3. E_s for $u_{j,m}(t)$, N=10,...,13. The graph of E_s for (12.1) for N=10,...,13. The horizontal axis is ϕ. Each curve represents the relative group speed error for the waves with wave number vector (ξ, η), $\xi h = \frac{2\pi}{N} \cdot \cos\phi$, $\eta h = \frac{2\pi}{N} \cdot \sin\phi$.

We now obtain our numerical computing scheme by ap-

proximating $\frac{d^2}{dt^2}u_{j,m}(t)$ using the second order centered finite difference method in time. Thus, using the notation $u^n_{j,m} \approx u_{j,m}(n\cdot\Delta t)$, we get

$$0 = c^2\cdot\left[\frac{u^n_{j+1,m} - 2\cdot u^n_{j,m} + u^n_{j-1,m}}{\Delta x^2} + \frac{u^n_{j,m+1} - 2\cdot u^n_{j,m} + u^n_{j,m-1}}{\Delta y^2}\right]$$

$$- \frac{u^{n+1}_{j,m} - 2\cdot u^n_{j,m} + u^{n-1}_{j,m}}{\Delta t^2}. \qquad (12.4)$$

Let us find a Fourier representation for $u^n_{j,m}$. Define

$$\hat{u}_n(\xi\Delta x, \eta\Delta y) = \Delta x\cdot\Delta y\cdot\sum_{m=-\infty}^{\infty}\sum_{j=-\infty}^{\infty} u^n_{j,m}\cdot e^{-i(\xi\Delta x\cdot j + \eta\Delta y\cdot m)}$$

where we think of the right side as the Fourier expansion for $\hat{u}_n$. Then,

$$u^n_{j,m} = \frac{1}{4\pi^2}\int_{-\pi/\Delta y}^{\pi/\Delta y}\int_{-\pi/\Delta x}^{\pi/\Delta x} \hat{u}_n(\xi\Delta x, \eta\Delta y)\cdot e^{i(\xi\Delta x\cdot j + \eta\Delta y\cdot m)}\, d\xi\, d\eta$$

where we need to find $\hat{u}_n$. Put this integral into (12.4) and use ideas from previous sections to obtain

$$0 = \left[\left(\frac{c}{\Delta x}\right)^2\cdot(e^{i\xi\Delta x} - 2 + e^{-i\xi\Delta x}) + \left(\frac{c}{\Delta y}\right)^2\cdot(e^{i\eta\Delta y} - 2 + e^{-i\eta\Delta y})\right]\hat{u}_n$$

$$- \frac{\hat{u}_{n+1} - 2\cdot\hat{u}_n + \hat{u}_{n-1}}{\Delta t^2}. \qquad (12.5)$$

Assume (12.5) has a solution of the form $A(\xi,\eta)\cdot z^n$ for

some complex function $z=z(\xi,\eta)$. Putting this into the above equation, we get

$$z - 2 + z^{-1} = \left[\frac{c\Delta t}{\Delta x}\right]^2(-4\cdot\sin^2\frac{\xi\Delta x}{2}) + \left[\frac{c\Delta t}{\Delta y}\right]^2(-4\cdot\sin^2\frac{\eta\Delta y}{2}). \quad (12.6)$$

If z solves (12.6), then so does z^{-1}. Thus, if $A\cdot z^n$ solves (12.5) then so does $B(\xi,\eta)\cdot z^{-n}$. Thus, $\hat{u}_n = A\cdot z^n + B\cdot z^{-n}$ is a general solution to (12.5) and

$$u^n_{j,m} = \frac{1}{4\pi^2}\int_{-\pi/\Delta y}^{\pi/\Delta y}\int_{-\pi/\Delta x}^{\pi/\Delta x} A(\xi,\eta)\cdot z^n\cdot e^{i(\xi\Delta x\cdot j+\eta\Delta y\cdot m)}\,d\xi\,d\eta$$

$$+ \frac{1}{4\pi^2}\int_{-\pi/\Delta y}^{\pi/\Delta y}\int_{-\pi/\Delta x}^{\pi/\Delta x} B(\xi,\eta)\cdot z^{-n}\cdot e^{i(\xi\Delta x\cdot j+\eta\Delta y\cdot m)}\,d\xi\,d\eta. \quad (12.7)$$

is a general solution to (12.4).

Claims 1 and 2 from section 4 must hold true for (12.6), except that we will require

$$\left[\frac{c\Delta t}{\Delta x}\right]^2 + \left[\frac{c\Delta t}{\Delta y}\right]^2 \le 1.$$

This will lead us to conclude that $|z|=1$. To see why the above is a sufficient requirement, we look first at (12.6). Recall from claim 2 of section 4 that for the sake of stability, we want to make sure (12.6) does not admit real solutions with absolute value different from 1. This amounted to making sure that the right side of (12.6) is always bounded below by -4 and above by 0. So, we have

$$-4 \le \left[\frac{c\Delta t}{\Delta x}\right]^2(-4\cdot\sin^2\frac{\xi\Delta x}{2}) + \left[\frac{c\Delta t}{\Delta y}\right]^2(-4\cdot\sin^2\frac{\eta\Delta y}{2}) \le 0$$

or

$$\left[\frac{c\Delta t}{\Delta x}\right]^2 + \left[\frac{c\Delta t}{\Delta y}\right]^2 \leq 1.$$

Thus, if z is a solution to (12.6), then z has the form

$$z = z(\xi,\eta) = e^{-i\omega\Delta t}$$

where $\omega=\omega(\xi,\eta)$. To determine ω, replace this exponential form for z in (12.7) and put this integral form into (12.4) to get

$$\omega = \pm\frac{1}{\Delta t}\cdot\cos^{-1}\left[\, 1 - 2\cdot\left[\left(\frac{c\Delta t}{\Delta x}\right)^2\cdot\sin^2\frac{\xi\Delta x}{2} + \left(\frac{c\Delta t}{\Delta y}\right)^2\cdot\sin^2\frac{\eta\Delta y}{2}\right]\right].$$

Define ω_1 to be the positive value of ω and ω_2 to be the negative value of ω. Thus,

$$u^n_{j,m} = \frac{1}{4\pi^2}\int_{-\pi/\Delta y}^{\pi/\Delta y}\int_{-\pi/\Delta x}^{\pi/\Delta x} A(\xi,\eta)\cdot e^{i(\xi\Delta x\cdot j+\eta\Delta y\cdot m-\omega_1\Delta t\cdot n)}\, d\xi\, d\eta$$

$$+ \frac{1}{4\pi^2}\int_{-\pi/\Delta y}^{\pi/\Delta y}\int_{-\pi/\Delta x}^{\pi/\Delta x} B(\xi,\eta)\cdot e^{i(\xi\Delta x\cdot j+\eta\Delta y\cdot m-\omega_2\Delta t\cdot n)}\, d\xi\, d\eta$$

is a general solution to (12.4).

Define [...] to be

$$\left(\frac{c\Delta t}{\Delta x}\right)^2\cdot\sin^2\frac{\xi\Delta x}{2} + \left(\frac{c\Delta t}{\Delta y}\right)^2\cdot\sin^2\frac{\eta\Delta y}{2}.$$

Then,

$$\Theta = \tan^{-1}\left|\frac{\Delta x}{\Delta y}\cdot\frac{\sin\eta\Delta y}{\sin\xi\Delta x}\right|$$

and

$$\left|\overline{C}_g\right| = \sqrt{\frac{c^4\cdot\Delta t^2}{\Delta x^2}\cdot\frac{\sin^2\xi\Delta x}{4([\ldots]-[\ldots]^2)} + \frac{c^4\cdot\Delta t^2}{\Delta y^2}\cdot\frac{\sin^2\eta\Delta y}{4([\ldots]-[\ldots]^2)}}\,.$$

Notice that Θ here is the same equation as (12.3). In fact, throughout the rest of this investigation, the approximation scheme continuous in time and the numerical computing scheme we get from it will always have the same group propagation angle equation. To simplify the analysis, we will let $h=\Delta x=\Delta y$. Thus, define [...] as

$$\sin^2\frac{\xi h}{2} + \sin^2\frac{\eta h}{2}$$

and $\nu = \frac{c\Delta t}{h}$, we get

$$|\phi-\Theta| = \left| \tan^{-1}\left|\frac{\eta}{\xi}\right| - \tan^{-1}\left|\frac{\sin\eta h}{\sin\xi h}\right| \right|$$

and

$$E_s = \left| \frac{1}{2}\cdot\sqrt{\frac{\sin^2\xi h+\sin^2\eta h}{[\ldots]-\nu^2[\ldots]^2}} - 1 \right|$$

where $\nu<\frac{\sqrt{2}}{2}$. Figure 12.4 is the graph of E_s for different values of N where $\nu=0.5$. At N=12, the curve lies within a 0.8 to 2.6% error span.

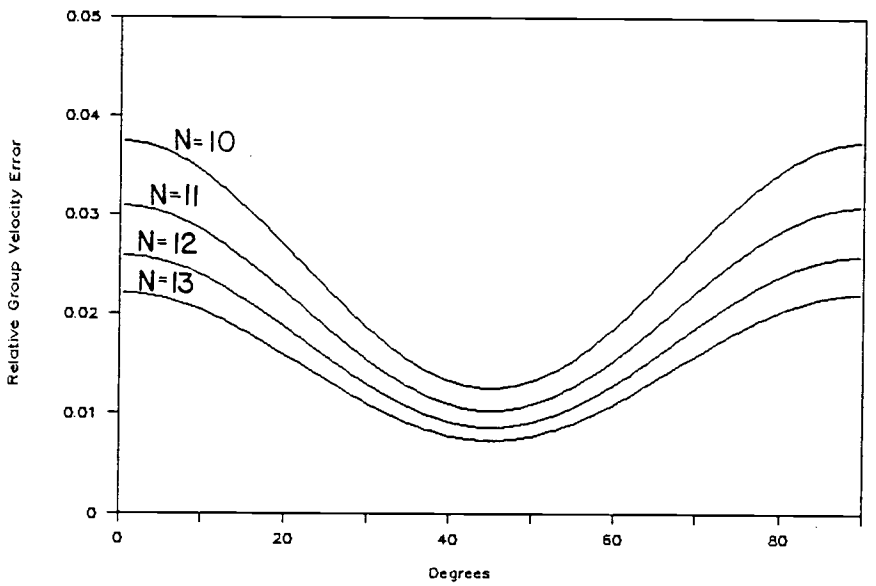

Figure 12.4. E_s for $u^n_{j,m}$, $\nu=0.5$, $N=10,\ldots,13$. The graph of E_s for (12.4) for $N=10,\ldots,13$ with $\nu=0.5$.

We will consider the test problem

$$u_{tt} = u_{xx} + u_{yy}$$

$$u(x,y,0) = e^{-500\{(x-2)^2+(y-2)^2\}}$$

$$u_t(x,y,0) = 0$$

$$u(0,y,t) = u(4,y,t) = u(x,0,t) = u(x,4,t) = 0$$

for $0<x<4$, $0<y<4$, and $t>0$.

Define $\Delta x=\Delta y=0.02$, $\Delta t=0.01$ and use (12.4) to approximate the solution to the test problem at t=2. Figure 12.5 is a graph of the numerical approximations at y=2 and

t=1.5. The shaded area of Figure 12.6 is the values for x and y where the numerical approximations are greater than 0.0001. Dispersion is occurring the most along the 0°, 90°, 180°, and 270° directions since this is where the shaded area of Figure 12.6 is thickest.

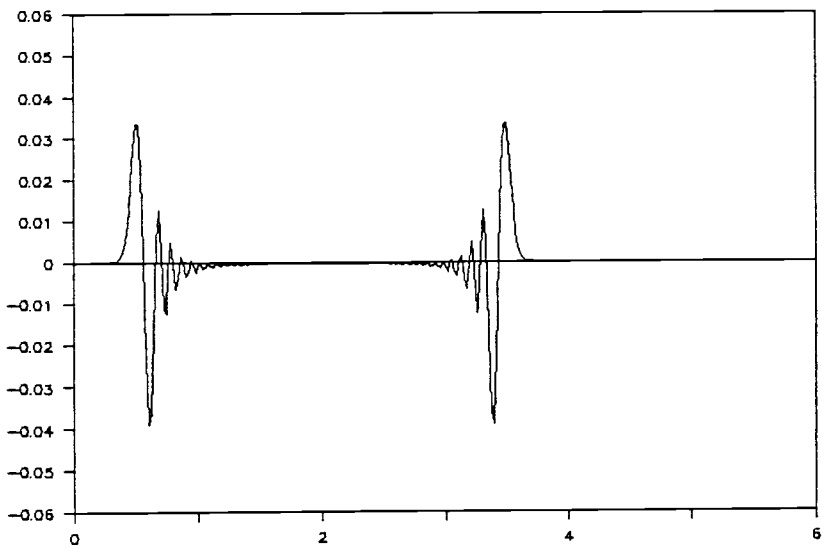

Figure 12.5. Test problem for $u^n_{j,m}$, ν=0.5, y=2. The graph of (12.4) for the test problem where ν=0.5, y=2, and n=149.

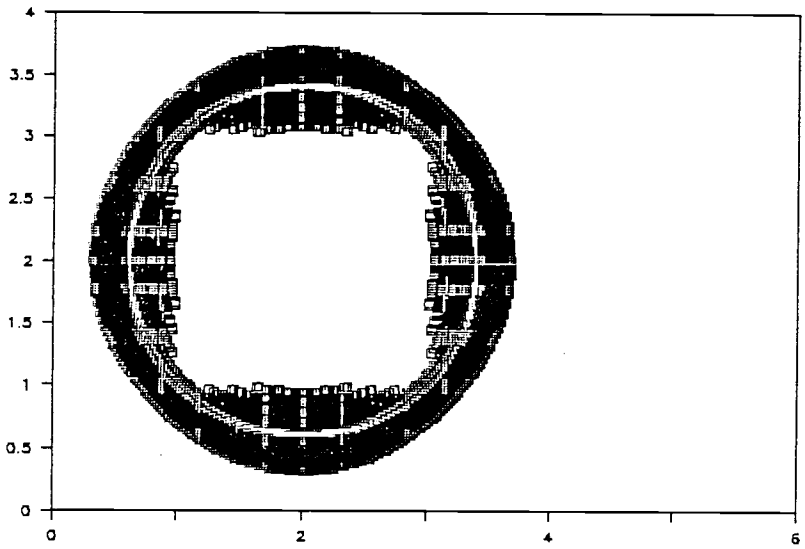

Figure 12.6. Domain of $u^n_{j,m}$ where $u^n_{j,m} > 0.0001$. The shaded area indicates where the numerical approximations from (12.4) are greater than 0.0001.

13. THE LINEAR FINITE ELEMENT METHOD IN 2-D

We will now use the linear finite element method in 2-D to approximate the spatial derivatives in the wave equation.

Define

$$\mathcal{L}[u] = c^2 \cdot (u_{xx} + u_{yy}) - u_{tt}.$$

We want to find u such that

$$\mathcal{L}[u] = 0$$

for the initial conditions

$$u(x,y,0) = f(x,y)$$

$$u_t(x,y,0) = g(x,y)$$

where $0<x<X$, $0<y<Y$, and $t>0$. As in the 1-D case, we will consider the convenient boundary conditions

$$u(0,y,t) = u(X,y,t) = u(x,0,t) = u(x,Y,t) = 0$$

for $t>0$.

If $\mathcal{L}[u]=0$, then

$$0 = \int_0^Y \int_0^X \mathcal{L}[u] \cdot w(x,y) \, dx\,dy$$

for any w. We can rewrite this as

$$0 = c^2 \cdot \int_0^Y \int_0^X u_{xx} \cdot w(x,y)\,dx\,dy + c^2 \cdot \int_0^Y \int_0^X u_{yy} \cdot w(x,y)\,dx\,dy$$

$$- \int_0^Y \int_0^X u_{tt} \cdot w(x,y)\,dx\,dy.$$

If w is continuously differeniable then use integration by parts on the inner integrals of the first two terms to get

$$
\begin{aligned}
0 \quad = \quad & c^2 \cdot \int_0^Y [\, u_x(X,y,t) \cdot w(X,y) - u_x(0,y,t) \cdot w(0,y) \,]\, dy \\
& - c^2 \cdot \int_0^Y \int_0^X u_x \cdot \frac{\partial}{\partial x} w \, dx\, dy \\
& + c^2 \cdot \int_0^X [\, u_y(x,Y,t) \cdot w(x,Y) - u_y(x,0,t) \cdot w(x,0) \,]\, dx \\
& - c^2 \cdot \int_0^X \int_0^Y u_y \cdot \frac{\partial}{\partial y} w \, dy\, dx \\
& - c^2 \cdot \int_0^Y \int_0^X u_{tt} \cdot w \, dx\, dy. \qquad (13.1)
\end{aligned}
$$

If (13.1) is satisfied for all w, then we can reverse the above argument to show that $\mathcal{L}[u] = 0$ (provided u_{xx} and u_{yy} both exist). Equation (13.1) is called the weak form of the PDE $\mathcal{L}[u] = 0$.

Divide [0,X] into R intervals of size Δx and [0,Y] into Q intervals of size Δy, and suppose that we approximate u with the piecewise linear function

$$\hat{u}(x,y,t) = \sum_{q=0}^{Q} \sum_{r=0}^{R} u_{r,q}(t) \cdot \psi_{r,q}(x,y)$$

where $\psi_{r,q}(x,y) = \phi_r(x) \cdot \phi_q(y)$, and $\{\phi_r\}$ and $\{\phi_q\}$ the linear finite element bases in x and y, respectively. We will set $u_{0,q}(t)$, $u_{R,q}(t)$, $u_{r,0}(t)$, and $u_{r,Q}(t)$ equal to zero so that $\hat{u}$ satisfies the boundary conditions. (For different boundary

conditions, these functions would not be set equal to zero.) Therefore, we approximate u by

$$\hat{u}(x,y,t) = \sum_{q=1}^{Q-1} \sum_{r=1}^{R-1} u_{r,q}(t) \cdot \psi_{r,q}(x,y).$$

Replace this representation for $\hat{u}$ into (13.1) and define $w(x,y)$ as $\psi_{j,m}$, $1 \le j \le R-1$ and $1 \le m \le Q-1$. Apply similar arguments from section 5 to get

$$\begin{aligned} 0 = {} & c^2 \cdot \sum_{q,r} u_{r,q}(t) \int_0^Y \int_0^X \frac{\partial}{\partial x}\psi_{r,q} \cdot \frac{\partial}{\partial x}\psi_{j,m} \, dx\,dy \\ & + c^2 \cdot \sum_{q,r} u_{r,q}(t) \int_0^Y \int_0^X \frac{\partial}{\partial y}\psi_{r,q} \cdot \frac{\partial}{\partial y}\psi_{j,m} \, dx\,dy \\ & + \sum_{q,r} u''_{r,q}(t) \cdot \int_0^Y \int_0^X \psi_{r,q} \cdot \psi_{j,m} \, dx\,dy. \end{aligned} \tag{13.2}$$

Consider the basis element $\psi_{j,m}$. Since $\psi_{j,m} = \psi_{j,m}(x,y) = \phi_j(x) \cdot \phi_m(y)$ where ϕ_j and ϕ_m are linear 1-D basis functions in x and y, respectively, the support for $\psi_{j,m}$ is the shaded region of Figure 13.1.

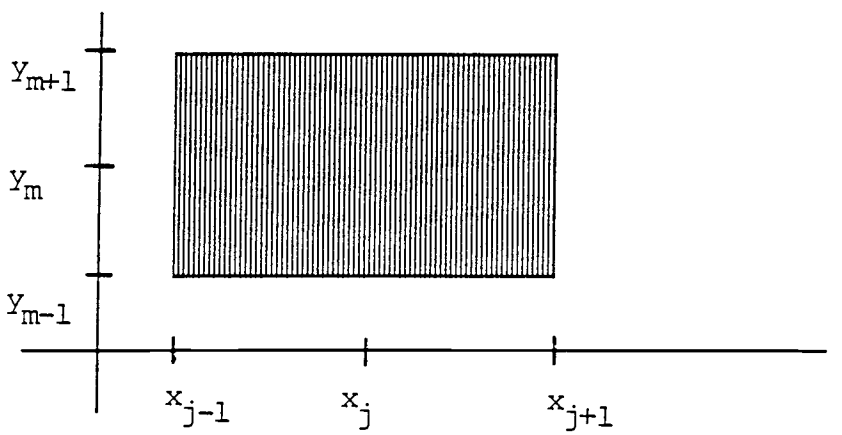

Figure 13.1. The support for $\psi_{j,m}$.

Thus, the only nonzero integrals of (13.2) are for $j-1 \le r \le j+1$ and $m-1 \le q \le m+1$. We evaluate a few of them. Consider the last term of (13.2). For r=j-1 and q=m-1, we have the integral

$$\int_0^Y \int_0^X \psi_{j-1,m-1} \cdot \psi_{j,m} \, dx\,dy = \int_0^X \phi_{j-1}(x) \cdot \phi_j(x) \, dx \cdot \int_0^Y \phi_{m-1}(y) \cdot \phi_m(y) \, dy$$

$$= \frac{\Delta x}{6} \cdot \frac{\Delta y}{6}$$

$$= \frac{\Delta x \cdot \Delta y}{36} .$$

When r=j and q=m-1, we have

$$\int_0^Y \int_0^X \psi_{j,m-1} \cdot \psi_{j,m} \, dx\,dy = \int_0^X \phi_j(x) \cdot \phi_j(x) \, dx \cdot \int_0^Y \phi_{m-1}(y) \cdot \phi_m(y) \, dy$$

$$= \frac{2\Delta x}{3} \cdot \frac{\Delta y}{6}$$

$$= \frac{\Delta x \cdot \Delta y}{9} .$$

When r=j+1 and q=m-1, we have

$$\int_0^Y \int_0^X \psi_{j+1,m-1} \cdot \psi_{j,m} \, dx\,dy = \int_0^X \phi_{j+1}(x) \cdot \phi_j(x) \, dx \cdot \int_0^Y \phi_{m-1}(y) \cdot \phi_m(y) \, dy$$

$$= \frac{\Delta x}{6} \cdot \frac{\Delta y}{6}$$

$$= \frac{\Delta x \cdot \Delta y}{36} .$$

Evaluate all the integrals in this fashion. Substitution

into (13.2) will give the 2-D linear finite element approximation scheme (we write $u_{j,m}(t)$ as $u_{j,m}$ for convenience)

$$
\begin{aligned}
c^2\cdot\Bigg(& \frac{u_{j-1,m-1} - 2\cdot u_{j,m-1} + u_{j+1,m-1}}{\Delta x^2} + 4\cdot\frac{u_{j-1,m} - 2\cdot u_{j,m} + u_{j+1,m}}{\Delta x^2} \\
& + \frac{u_{j-1,m+1} - 2\cdot u_{j,m+1} + u_{j+1,m+1}}{\Delta x^2}\Bigg) \\
+ \; c^2\cdot\Bigg(& \frac{u_{j-1,m-1} - 2\cdot u_{j-1,m} + u_{j-1,m+1}}{\Delta y^2} + 4\cdot\frac{u_{j,m-1} - 2\cdot u_{j,m} + u_{j,m+1}}{\Delta y^2} \\
& + \frac{u_{j+1,m-1} - 2\cdot u_{j+1,m} + u_{j+1,m+1}}{\Delta y^2}\Bigg) \\
= \; \tfrac{1}{2}\Bigg(& (\tfrac{1}{6}u''_{j-1,m-1} + \tfrac{2}{3}u''_{j,m-1} + \tfrac{1}{6}u''_{j+1,m-1}) + 4\cdot(\tfrac{1}{6}u''_{j-1,m} + \tfrac{2}{3}u''_{j,m} + \tfrac{1}{6}u''_{j+1,m}) \\
& + (\tfrac{1}{6}u''_{j-1,m+1} + \tfrac{2}{3}u''_{j,m+1} + \tfrac{1}{6}u''_{j+1,m+1})\Bigg) \\
+ \tfrac{1}{2}\Bigg(& (\tfrac{1}{6}u''_{j-1,m-1} + \tfrac{2}{3}u''_{j-1,m} + \tfrac{1}{6}u''_{j-1,m+1}) + 4\cdot(\tfrac{1}{6}u''_{j,m-1} + \tfrac{2}{3}u''_{j,m} + \tfrac{1}{6}u''_{j,m+1}) \\
& + (\tfrac{1}{6}u''_{j+1,m-1} + \tfrac{2}{3}u''_{j+1,m} + \tfrac{1}{6}u''_{j+1,m+1})\Bigg)
\end{aligned}
\tag{13.3}
$$

It looks as though we obtained (13.3) in the following way. First, we fix the y variable in the 2-D wave equation at the point $y=y_{m-1}$ and apply the 1-D linear finite element method in x to it. Do the same thing for y fixed at

$y=y_m$ and y_{m+1}. Next, fix the x variable in the wave equation at the points $x=x_{j-1}$, x_j, and x_{j+1} and at each fixed point, apply the 1-D linear finite element method in y to it. We now have six different equations. Take a weighted average of these six and we get (13.3). We define (13.3) as a 1-4-1 averaging of the 1-D linear finite element approximation. The graphs of $|\Theta-\phi|$ for (13.3) looks very similar to the graph of $|\Theta-\phi|$ for (12.1). For the sake of brevity, the graphs are not shown here. At N=12, the graphs are within 0.29° of each other, both having an error of no more than 0.69°. For E_s for (13.3), the graph corresponding to N=12 lies within a 1.7 to 3.4% error region. This is the same result we got from the graph of E_s for (12.1). The graphs for E_s for (13.3) and (12.1) overlap for N greater than or equal to 12.

To use (13.3) to obtain a numerical computing scheme would be difficult. To simplify things, we will replace the entire right side of (13.3) with $u''_{j,m}$ (i.e., we will mass lump the right side of (13.3) by replacing it with $u''_{j,m}$). Label this new scheme (13.4) and call it the 2-D unweighted linear finite element approximation scheme. The graphs of $|\Theta-\phi|$ for (13.4) looks very much like the graphs for (13.3) and (12.1). At N=12, the graph of $|\Theta-\phi|$ for (13.4) never exceeds 0.70°. The graphs of E_s for (13.4) looks much worse than the graph of E_s for (13.3) and

(12.1). The graph of E_s for (13.4) with N=12 lies within a 3.5 to 5.0% error region.

Approximate $u''_{j,m}$ of (13.4) in the usual way to get the numerical computing scheme. Label this scheme (13.5). For $\nu = \frac{c\Delta t}{h}$, where $h = \Delta x = \Delta y$, we require $\nu < 1$. This is determined by experimentation and not analysis because (13.5) is too difficult to deal with. Consider E_s for (13.5) with $\nu = 0.5$. The curve for N=12 lies within a 2.6 to 4.4% error range. This result is much worse than E_s for (12.4) with the same value for ν. Thus, on the basis of their relative group speed error results, (13.5) will not be as accurate a numerical computing scheme as (12.4) when $\nu = 0.5$.

14. THE REVISED LINEAR FINITE ELEMENT METHOD IN 2-D

Consider (13.2) where $\psi_{r,q}=\phi_r(x)\cdot\phi_q(y)$ and $\psi_{j,m} = \phi_j(x)\cdot\phi_m(y)$. We define, in this case, $\{\phi_r\}$, $\{\phi_q\}$, $\{\phi_j\}$, and $\{\phi_m\}$ as the 1-D quadratic finite element bases in x or y, appropriately. Recall from section 6 that the graph of ϕ_j depend on if j is odd or even. Because of this, the quadratic finite element approximation scheme will be a multiple equation scheme, each scheme being indexed in (j,m); j even m even, j odd m even, j even m even, and j even m even. In the 1-D case, we ended up with a quadratic finite element approximation scheme composed of two equations. We were forced to skip all analysis and had to settle with just looking at a graph of its numerical approximations at a fixed time point. In this case, we are in the same predicament except we will not even attempt to get numerical approximations using the quadratic finite element method. The difficulty involved in programming any computing scheme we obtain would be too great.

In the 1-D quadratic finite element approximation scheme, we had two equations subscripted in j, one for j odd and the other for j even. We defined the revised linear finite element approximation scheme by considering the equation for j odd and redefining it for all integer values of j. We will do something similar to develop the

revised linear finite element approximation in 2-D. Once again, consider (13.2) where $\psi_{r,q}=\psi_{r,q}(x,y)=\phi_r(x)\cdot\phi_q(y)$ and $\psi_{j,m}=\psi_{j,m}(x,y)=\phi_j(x)\cdot\phi_m(y)$. Define ϕ_r, ϕ_q, ϕ_j, ϕ_m as the 1-D quadratic finite element bases in x and y, appropriately. In this case, we will fix j and m as odd integers. Evaluate each integral and the equation we end up with will be one of the equations that make up the quadratic finite element approximation scheme in 2-D. At this point, define this equation for all integers j and m and define it as the revised linear finite element approximation scheme in 2-D.

We proceed as discussed. For (13.2), define $\psi_{r,q}=\phi_r(x)\cdot\phi_q(y)$ and $\psi_{j,m}=\phi_j(x)\cdot\phi_m(y)$ where ϕ_r, ϕ_q, ϕ_j, and ϕ_m are the 1-D quadratic finite element bases in x and y, appropriately. Fix j and m as odd integers. Thus, $\psi_{j,m}$ has the same support of the form drawn in section 13 when we were discussing the linear finite element basis. Thus, the only nonzero integrals in (13.2) are found when $j-1\le r\le j+1$ and $m-1\le q\le m+1$. We evaluate the integral of the first term of (13.2), r=j-1 and q=m-1,

$$\int_0^Y \int_0^X \psi_{j-1,m-1}\cdot\psi_{j,m}\,dx\,dy = \int_0^X \phi_{j-1}(x)\cdot\phi_j(x)\,dx\cdot\int_0^Y \phi_{m-1}(y)\cdot\phi_m(y)\,dy$$

$$= \frac{2\Delta x}{15}\cdot\frac{2\Delta y}{15}$$

$$= \frac{4}{225}\Delta x\cdot\Delta y\,.$$

For r=j and q=m-1, we have

$$\int_0^Y \int_0^X \psi_{j,m-1} \cdot \psi_{j,m} \, dx dy = \int_0^X \phi_j(x) \cdot \phi_j(x) \, dx \cdot \int_0^Y \phi_{m-1}(y) \cdot \phi_m(y) \, dy .$$

$$= \frac{16\Delta x}{15} \cdot \frac{2\Delta y}{15}$$

$$= \frac{32}{225} \Delta x \cdot \Delta y .$$

The rest of the integrals are evaluated in a similar fashion. Replace these values into (13.2), define it for all values of j and call this equation the revised linear finite element approximation scheme in 2-D. Label it as (14.1). We end up with a scheme that is a 1-8-1 averaging of the 1-D revised linear finite element approximation at the points $y=y_{m-1}$, y_m, y_{m+1} and $x=x_{j-1}$, x_j, x_{j+1}. At N=12, the propagation angle error never exceeds 0.12° and the relative speed error curve lies within a 0.3 to 0.6% interval.

To obtain a numerical computing scheme from (14.1), we convert it to an unweighted scheme as we did in the true 2-D linear finite element approximation scheme. Call this the 2-D unweighted revised linear finite element approximation scheme and label it (14.2). The propagation angle for (14.2) is at about the same level of accuracy as (14.1) but the relative speed is much worse. At N=12, $|\Theta-\phi|$ for (14.2) never exceeds 0.13% . At N=12, E_s has risen

between a 3.5 to 3.7% region. A very important observation of the relative group speed error graphs is that the curves are almost flat, i.e., (14.2) is a near isotropic scheme. We interpret what this means. Consider the solution to the wave equation, u and the solution to (14.2), $u_{j,m}(t)$. We can imagine u to be a superposition of travelling waves, all of which have group speed |c| no matter what its group propagation angle is. Now, consider $u_{j,m}(t)$. By its relative group speed error graphs, it is composed of a superposition of travelling waves that all travel at about the same speed. Although the error in speed is relatively high, it is at least a uniform error no matter what the angle is.

Convert (14.2) into a numerical computing scheme and call it (14.3). Some experimenting shows that we must require $\nu < \sqrt{\frac{5}{6}}$. The graphs of E_s for (14.3) when $\nu = 0.5$ are about as good as for previous sections but the near isotropic behavior from (14.3) is still quite obvious. At N=12, the graph for E_s for (14.3) lies in a 2.55 to 2.9% range.

15. THE FOURTH ORDER CENTERED FINITE DIFFERENCE METHOD IN 2-D

Consider the 2-D wave equation. Approximate u_{xx} using the fourth order centered finite difference method by expanding along the line $y=y_m$. Similarly, approximate u_{yy} using the fourth order method on the line $x=x_j$. Thus, we get the fourth order centered finite difference approximation scheme

$$c^2\cdot\left[\frac{4}{3}\cdot\frac{u_{j+1,m}(t)-2\cdot u_{j,m}(t)+u_{j-1,m}(t)}{\Delta x^2}-\frac{1}{12}\cdot\frac{u_{j+2,m}(t)-2\cdot u_{j,m}(t)+u_{j-2,m}(t)}{\Delta x^2}\right]$$

$$+\ c^2\cdot\left[\frac{4}{3}\cdot\frac{u_{j,m+1}(t)-2\cdot u_{j,m}(t)+u_{j,m-1}(t)}{\Delta y^2}-\frac{1}{12}\cdot\frac{u_{j,m+2}(t)-2\cdot u_{j,m}(t)+u_{j,m-2}(t)}{\Delta y^2}\right]$$

$$=\frac{d^2}{dt^2}u_{j,m}(t)\,. \qquad (15.1)$$

Figures 15.1 and 15.2 give the graphs of $|\Theta-\phi|$ and E_s for (15.1). The results are a great deal better than for previous schemes. At N=12, the curve for the propagation angle error does not exceed 0.035° and at N=12, the curve for the relative speed error is at most 0.2%.

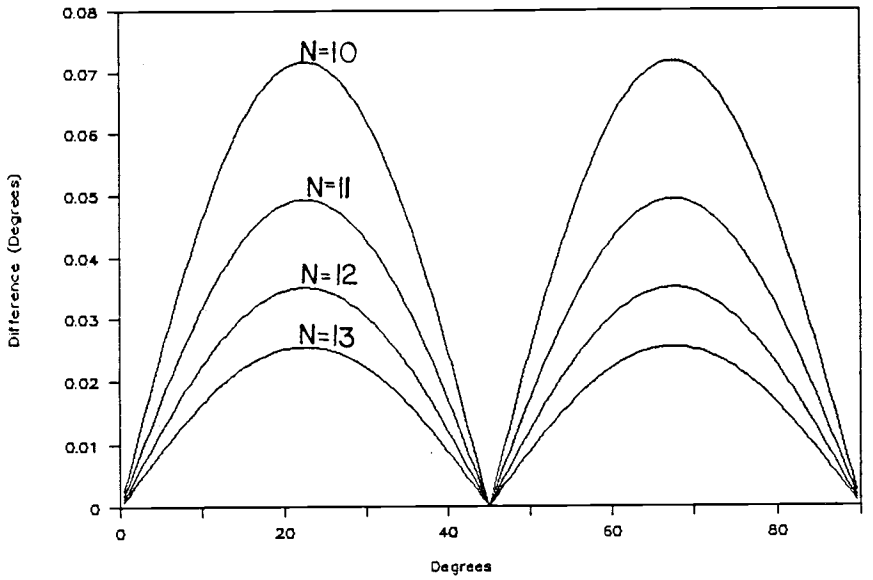

Figure 15.1. $|\Theta-\phi|$ for $u_{j,m}(t)$, N=10,...,13. The graph of $|\Theta-\phi|$ for (15.1) for N=10,...,13.

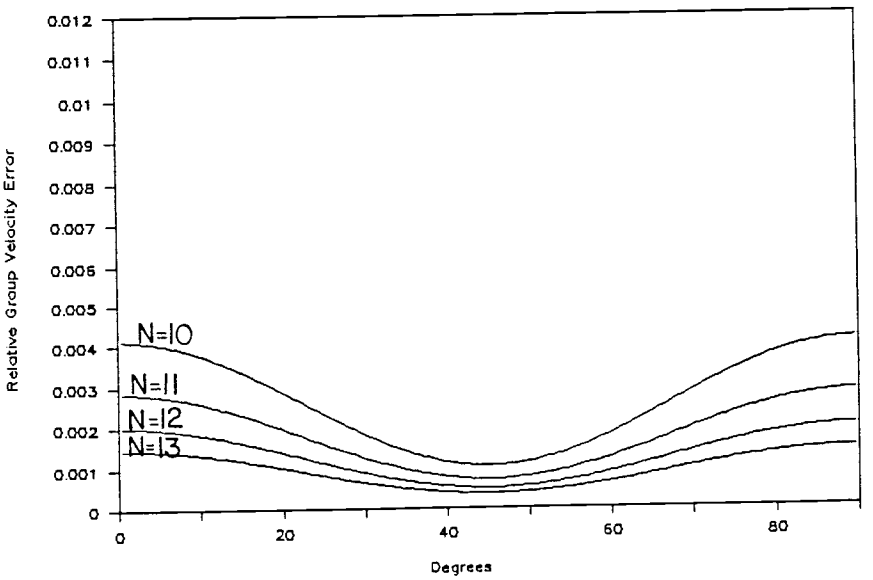

Figure 15.2. E_s for $u_{j,m}(t)$, N=10,...,13. The graph of E_s for (15.1) for N=10,...,13.

Obtain the numerical computing scheme from (15.1) in the usual way and call this new scheme (15.2). In this case, we find experimentally that $\nu < \sqrt{\frac{3}{8}}$. When $\nu = 0.5$, the graph of the relative speed error for N=12 lies in the region 0.66 to 0.82%. This is the best result we have seen so far for a fully discretized scheme. See Figure 15.3.

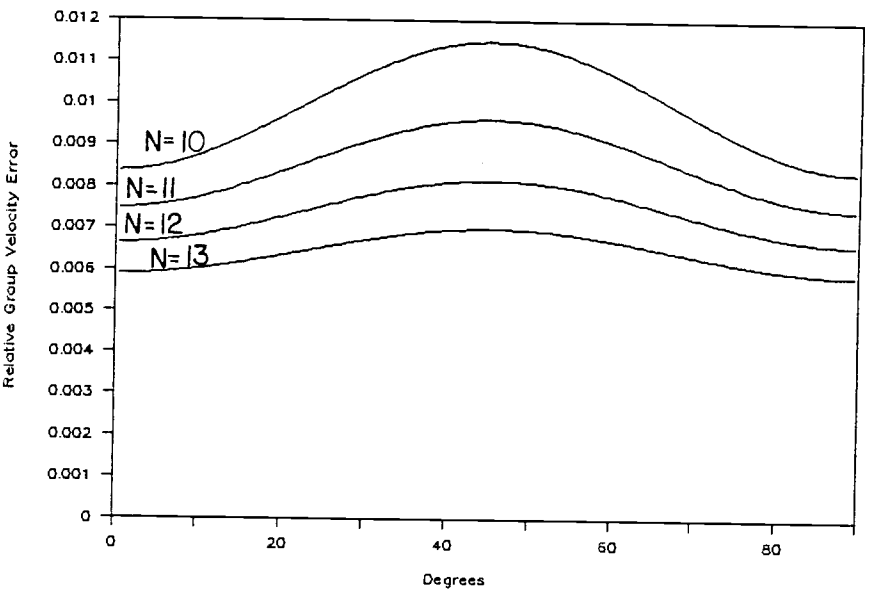

Figure 15.3. E_s for $u^n_{j,m}$, $\nu=0.5$, N=10,...,13. The graph of E_s for (15.2) for N=10,...,13 with $\nu=0.5$.

The final two approximation methods are studied in the hope of finding a near isotropic approximation scheme. They will both be variations on (15.1).

We start by developing a diagonal fourth order cen-

tered finite difference approximation scheme. To obtain this scheme, we will use the fact that the Laplacian is invariant under rotated coordinates. This means that if we consider the rotated coordinates x' and y' at the point (x,y) (in this case, we will rotate it by 45°) then $u_{xx}+u_{yy} = u_{x'x'}+u_{y'y'}$, see Figure 15.4.

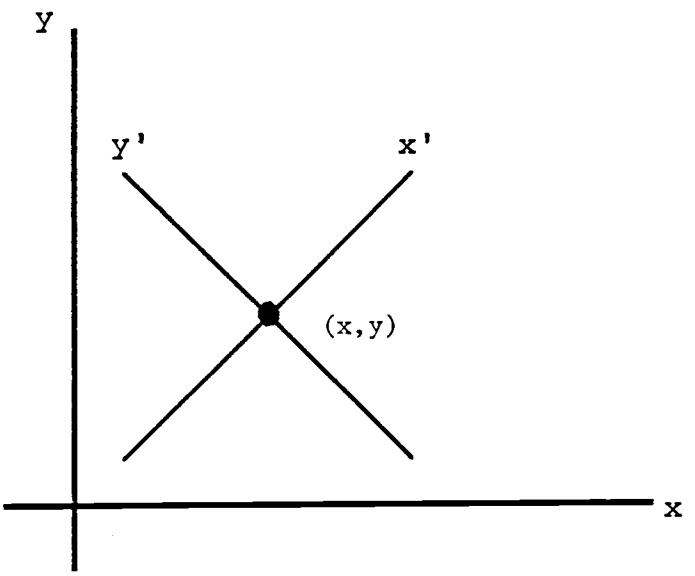

Figure 15.4. The x'-y' coordinate axis. We obtain them by rotating the x-y coordinate axis 45°at the point (x,y).

To approximate $u_{x'x'}$ at the point (x_j,y_m), we will expand along the x' axis using the fourth order centered finite difference method and the points indicated in Figure 15.5. To approximate $u_{y'y'}$ at the point (x_j,y_m), we will expand along the y' axis using the fourth order centered finite difference method and the points indicated in Figure 15.6.

The step size we are now using is $\sqrt{\Delta x^2 + \Delta y^2}$.

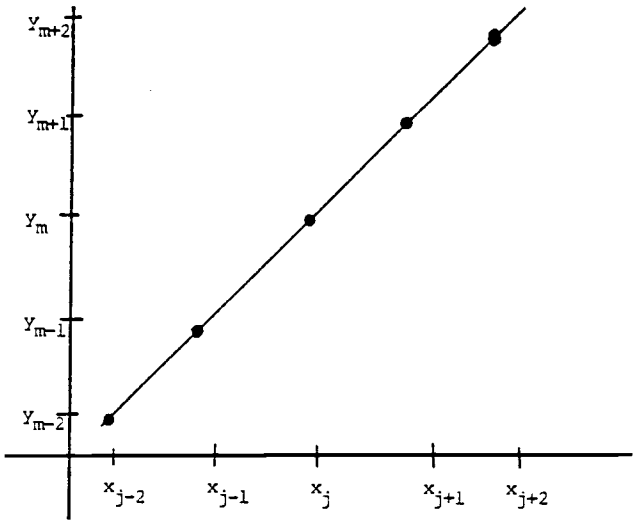

Figure 15.5. The points on the x'-axis used to approximate $u_{x'x'}$ at (x_j, y_m).

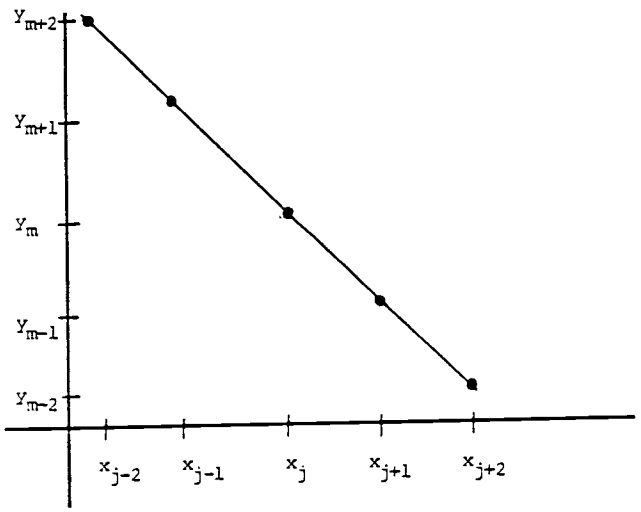

Figure 15.6. The points on the y'-axis used to approximate $u_{y'y'}$ at (x_j, y_m).

Thus, the 2-D diagonal fourth order centered finite difference approximation scheme is

$$c^2\cdot\left(\frac{4}{3}\cdot\frac{u_{j+1,m+1}(t)-2\cdot u_{j,m}(t)+u_{j-1,m-1}(t)}{\Delta x^2+\Delta y^2}\right.$$

$$\left.-\frac{1}{12}\cdot\frac{u_{j+2,m+2}(t)-2\cdot u_{j,m}(t)+u_{j-2,m-2}(t)}{\Delta x^2+\Delta y^2}\right)$$

$$+\ c^2\cdot\left(\frac{4}{3}\cdot\frac{u_{j+1,m-1}(t)-2\cdot u_{j,m}(t)+u_{j-1,m+1}(t)}{\Delta x^2+\Delta y^2}\right.$$

$$\left.-\frac{1}{12}\cdot\frac{u_{j+2,m-2}(t)-2\cdot u_{j,m}(t)+u_{j-2,m+2}(t)}{\Delta x^2+\Delta y^2}\right)$$

$$=\frac{d^2}{dt^2}u_{j,m}(t)\,. \qquad (15.3)$$

The graphs of $|\Theta-\phi|$ and E_s for (15.3) indicate that (15.3) is not quite as good a scheme as (15.1) but much better than all the previous ones. In any case, the graphs for E_s indicate that we do not have an isotropic scheme. The fact that (15.3) does not yield as good results as (15.1) should not be too surprising. This is because in the case of (15.3), we are using a step size of $\sqrt{2}\cdot h$ instead of just h where $h=\Delta x=\Delta y$. The bigger step size is the probable reason for (15.3) not being as accurate as (15.1).

Call (15.4) the numerical computing scheme for (15.3). In this case, we find that $\nu<\frac{\sqrt{3}}{2}$. The graphs of E_s for various values of N with $\nu=0.5$ look better than the

results from all previous schemes except (15.2). Once again, no isotropic behavior is observed.

Finally, let us consider taking an average of (15.1) and (15.3). Call this scheme the combined fourth order centered finite difference approximation scheme. Label it (15.5). A bit of experimentation shows that we must restrict $\nu < \frac{\sqrt{2}}{2}$. The results for its group propagation angle and group speed is an averaging of the results from (15.1) and (15.3), which is not surprising. Obtaining and analyzing the numerical computing scheme gotten from (15.5) would be very difficult and since (15.5) does not appear to be more accurate nor isotropic an approximation scheme than (15.1), we will not go any further with this.

Recall the test problem from section 12. Figures 15.7 and 15.8 are the numerical results using (15.2). Figure 15.7 is a graph of the numerical results when y=2 and t=1.5. The shaded area in Figure 15.8 indicates where the numerical approximations of (15.2) are greater than 0.0001. Notice how much more circular the shaded region is compared to Figure 12.6. This tells us that there is less dispersion occurring when (15.2) is used than when (12.4) is used.

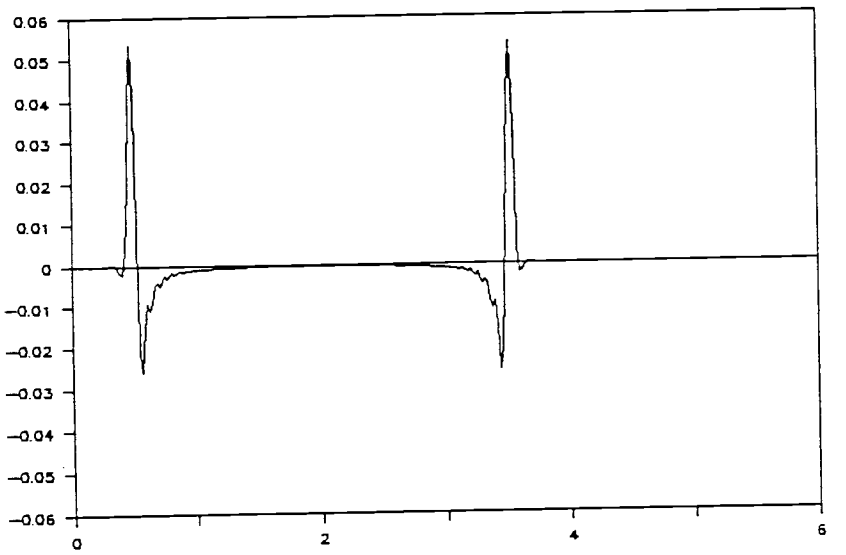

Figure 15.7. Test problem for $u^n_{j,m}$, ν=0.5, y=2. The graph of the numerical approximations for y=2, t=1.5. The graph shows how much less dis-persion is occurring when compared to Figure 12.5.

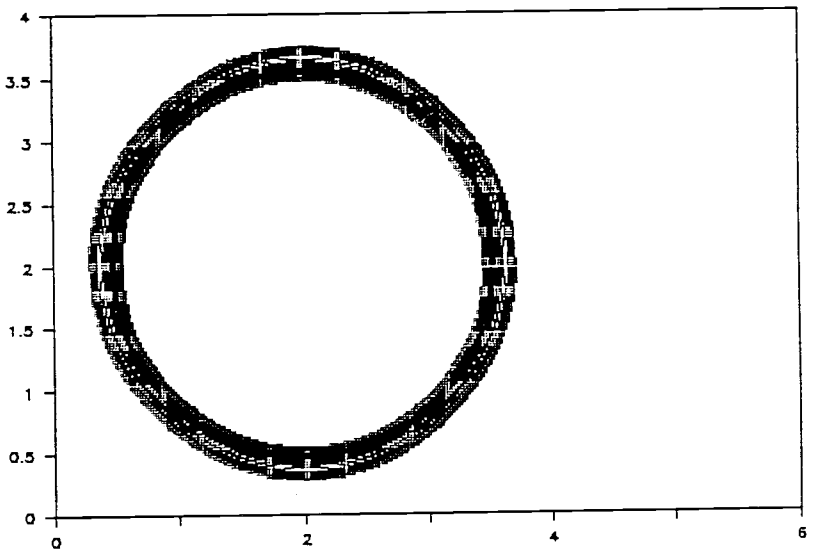

Figure 15.8. Domain of $u^n_{j,m}$ where $u^n_{j,m} > 0.0001$. The shaded area indicates where the numerical approximations of (15.2) are greater than 0.0001. The circular, thin region indicates that (15.2) is a less dispersive computing scheme than scheme (12.4).

16. SUMMARY FOR THE 2-D CASE

Consider the time continuous approximation schemes obtained by implementing the following approximation methods.

1. The second order centered finite difference method (label this scheme as FD2)
2. The linear finite element method (LFEM)
3. The revised linear finite element method (RLFEM)
4. The unweighted linear finite element method (ULFEM)
5. The unweighted revised linear finite element method (URLFEM)
6. The fourth order centered finite difference method (FD4)
7. The diagonal fourth order centered finite difference method (DFD4)

Label the scheme obtained by averaging FD4 and DFD4 as CFD4.

We can divide these eight schemes into two groups according to their degree of accuracy.

1. FD2
2. LFEM
3. ULFEM

4. URLFEM

and

1. RLFEM
2. FD4
3. DFD4
4. CFD4

Consider the first group. The LFEM was a disappointment because it gave such a complicated formula with an accuracy no better than FD2, whereas FD2 was a much simpler one. Mass lumping was used to obtain the schemes ULFEM and URLFEM. They came about because of the complications involved in trying to obtain numerical computing schemes from LFEM and the RLFEM. Much of the accuracy of RLFEM was lost when we obtained URLFEM but the appealing thing about URLFEM was its near isotropic behavior. Less isotropic behavior was observed in ULFEM and its accuracy level compared to URLFEM was much worse.

The accuracy level of the second group is far better than the accuracy level of the first group with FD4 being the best of them. As in the 1-D case, RLFEM was a surprise; although a very complicated scheme, its accuracy level puts it in the same level as the schemes with fourth order accuracy. Scheme DFD4 had an accuracy level comparable to FD4 but DFD4 does not seem to offer any advantage that FD4 already has. The scheme CFD4 is not worth using

because of its complexity and because its accuracy level is merely an averaging of the accuracy levels of FD4 and DFD4.

Next, consider the numerical computing schemes obtained from the above time continuous approximation schemes. We will keep the same labels. We group them by their degree of accuracy.

1. FD2
2. URLFEM
3. ULFEM

and

1. FD4
2. DFD4

Approximating $u_{j,m}''(t)$ with

$$\frac{u_{j,m}^{n+1} - 2 \cdot u_{j,m}^{n} + u_{j,m}^{n-1}}{\Delta t^2}$$

will have an overall effect on the degree of accuracy in the numerical computing scheme obtained. Using another approximation form for $u_{j,m}''(t)$ could change our results quite a bit. The advantage in using the above approximation for $u_{j,m}''(t)$ is that all five of the numerical computing schemes are explicit schemes. Of the five, FD4 is the most accurate scheme but if only rough estimates are needed, URLFEM should be used because of its simpler nature and its near isotropic behavior.

17. BIBLIOGRAPHY

[1] Fletcher, C.A.J. *Computational Galerkin Methods*. New York : Springer-Verlag, 1984.

[2] Lapidus, L. and Pinder, G.F. *Numerical Solution Of Partial Differential Equations In Science And Engineering*. New York : Wiley, 1982.

[3] Lighthill, J. *Waves In Fluids*. New York : Cambridge University Press, 1978.

[4] Shubin, G.R. and Bell, J.B. "A Modified Equation Approach To Constructing Fourth Order Methods For Acoustic Wave Propagation", *SIAM J. Sci. Stat. Comput.*, Vol.8, No.2, 1987, pp.135-150.

[5] Strang G. and Fix, G.J. *An Analysis Of The Finite Element Method.* New Jersey : Prentice Hall, 1973.

[6] Trefethen, L.N. "Group Velocity In Finite Difference Schemes", *SIAM Review*, Vol.24, No.2, 1982, pp.113-136.

[7] Whitham, G. *Linear And Nonlinear Waves.* New York : Wiley-Interscience, 1974.